ADVANCES IN PHYSICS, 1981, VOL. 30, NO. 4, 475–538

Optically detected magnetic resonance (O.D.M.R.) investigations of recombination processes in semiconductors†

By B. C. CAVENETT

Department of Physics, University of Hull, Hull, England

[Received 12 February 1981]

ABSTRACT

This review covers results of recent O.D.M.R. measurements of recombination processes in layered semiconductors, II–VI compounds, at dep traps and in amorphous compounds, and includes consideration of experimental aspects.

CONTENTS

† Based on unpublished invited paper presented at the International Conference on High Magnetic Field Measurements in Semiconductors, Oxford, 1978.

0001–8732/81/3004 0475 $02·00

§ 1. Introduction to optical resonance techniques

The application of optically detected magnetic resonance (O.D.M.R.) to the investigations of luminescence processes in solids is now well established. These techniques were developed from optical pumping studies in gases by Geschwind *et al.* [1, 2] who investigated chromium in Al_2O_3 and since then a wide variety of problems has been studied. The early results of investigations of magnetic ions in insulators have been reviewed by Geschwind [3], whereas details of more recent studies can be found in the review by Henderson [4].

The use of optical pumping and optical resonance methods to study recombination radiation in semiconductors has developed rapidly over recent years and the early work can be found in the reviews by Zakharchenya [5–7], Lampel [8], Planel [9], Davies [10], Davies *et al.* [11] and Cavenett [12–14]. It is the purpose of this paper to summarize the present state of the subject and to show that O.D.M.R. has many advantages for studies of electron–hole recombination processes in both crystalline and amorphous semiconductors.

Conventional E.P.R. techniques have been used very successfully to study defect and impurity centres in semiconductors for many years. Early results have been reviewed by Ludwig and Woodbury [15], Title [16] and Lancaster [17] while more recently work on III–V compounds has been reviewed by Varshni [18], defects in II–VI compounds by Schneider [19], amorphous semiconductors by Bishop *et al.* [20] and Solomon [21], heavily doped semiconductors by Morigaki [22] and defects in III–V semiconductors by Kaufmann and Schneider [23]. Watkins [24] has reviewed in considerable detail the investigations of radiation-induced defects in silicon.

In a conventional resonance experiment the sample is placed in a microwave capacity and a magnetic field is applied to the sample such that $B_{\text{r.f.}}$ is normal to B_{ext}. The ground state will be in thermal equilibrium and so, when the microwave energy equals the separation between the Zeeman electronic levels of the magnetic ion or defect, resonant absorption of microwave power occurs and is measured by using a microwave bridge. For a detailed discussion of the principles of E.P.R. see Abragam and Bleaney [25] and for a summary of the techniques see, for example, Poole [26]. In the optical resonance experiments the sample is also placed in a microwave cavity but luminescence is excited by a laser and microwave induced changes in the luminescence intensity or polarization of the emission are detected at resonance.

At present there are two optical magnetic resonance techniques which are being used to investigate semiconductors. One is called optical pumping or conduction electron–spin resonance (C.E.S.R.) since this technique has been used to determine the conduction band g-factors in pure and alloy semiconductors. In these experiments which have been reviewed by Lampel [8] and Planel [9] population differences between the Zeeman levels of the conduction electrons are induced by pumping with circularly polarized light near the band gap energy. The resulting electronic polarization produces, in turn, an emission polarization and so magnetic resonance can be detected as a decrease in emission polarization. More details are given in § 2. The second technique is simply known as optically detected magnetic resonance (O.D.M.R.) and its success depends on there being sufficiently large population differences between the magnetic sublevels as a result either of thermalization or because different decay rates from the various sublevels preferentially empty the strongly emitting states. At resonance non-emitting states are converted to emitting states and so the emission intensity increases. These two techniques are, of course,

quite complementary since if we write the electronic polarization of a spin doublet as

$$P=\frac{n_+-n_-}{n_++n_-}, \tag{1.1}$$

where n_+, n_- are the populations of the $M_S=+\frac{1}{2}$, $-\frac{1}{2}$ states, respectively, then, if T_1 is the spin lattice relaxation time and τ is the optical lifetime, we have

$$P=P_{\mathrm{i}}\frac{T_1}{T_1+\tau}+P_{\mathrm{T}}\frac{\tau}{T_1+\tau}, \tag{1.2}$$

where P_{i} is the maximum electronic polarization produced by optical pumping (see §2) and P_{T} is the maximum thermal polarization given by the expression $P_{\mathrm{T}}=P_0\tanh(g\mu_{\mathrm{B}}B/2kT)$. If $T_1\gg\tau$ then $P=P_{\mathrm{i}}$ and the optical pumping experiment can achieve large electronic polarizations (though one should remember that even in this case O.D.M.R. is possible without optical pumping if the decay rates from the Zeeman levels are unequal as discussed previously). In the case where $\tau\gg T_1$ we have $P=P_{\mathrm{T}}$ and only the O.D.M.R. experiment is appropriate. However, in general, the excited states of defects in semiconductors have T_1 and τ which do not correspond to the extreme cases outlined above so that the O.D.M.R. experiment combined with optical pumping can be used with considerable success to characterize a particular recombination process. This combined technique was first used by Dawson *et al.* [27] for an investigation of exciton recombination processes in CdS.

In the case of the O.D.M.R. experiments the effect of the microwaves on the luminescence can most easily be seen if we consider the examples shown in fig. 1. In the first example, fig. 1 (*a*), donor–acceptor recombination in CdS is shown, where the donor state is described by $S=\frac{1}{2}$ from the almost isotropic conduction band and the acceptor state is derived from the uppermost valence band ($J=\frac{3}{2}$ with spin–orbit

Fig. 1

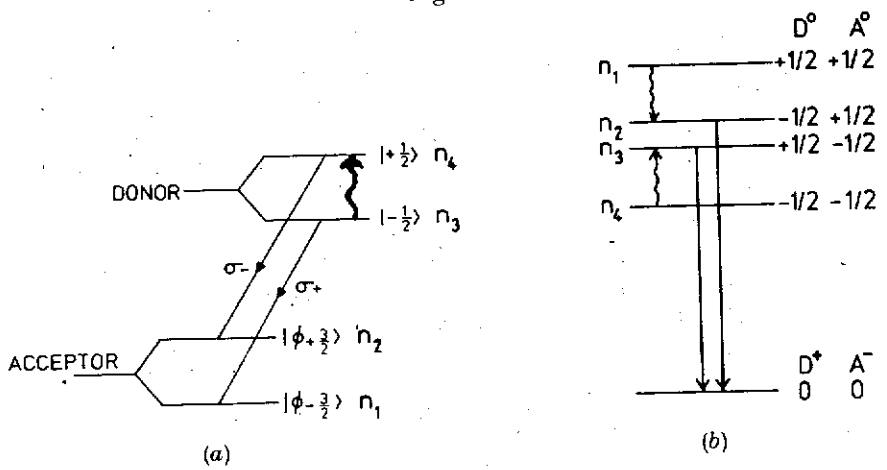

(*a*) Magnetic resonance in the thermalized donor state of a donor–acceptor pair. At resonance $I_{\sigma-}$ increases and $I_{\sigma+}$ decreases. (*b*) Allowed singlet recombination depletes the populations n_2, n_3 for an unthermalized donor–acceptor pair and resonance of the donors increases the total intensity of the luminescence.

interaction and axial symmetry). The allowed emissions are circularly polarized when viewed along the magnetic field direction for $B \| c$-axis. If the donor is thermalized with $n_3 > n_4$, resonance will occur as shown from $n_3 \rightarrow n_4$ increasing the intensity of $\sigma-$ and decreasing $\sigma+$. The maximum signal at 9 GHz is approximately 0·1% and little or no signal is observed if the total emission is monitored instead of one of the circularly polarized components. The second case shown in fig. 1 (*b*) is that of a weakly exchange coupled donor–acceptor pair which is unthermalized. For ZnS or ZnSe the donor states are described by $M_S = \pm\frac{1}{2}$ and for a deep acceptor the unpaired spin is also described by $S = \frac{1}{2}$. Therefore, in the magnetic field the levels are as shown and the allowed emission is from the singlet excited state to the singlet ground state. For an unthermalized system, levels n_2 and n_3 are emptied by the allowed emission process and at resonance the total emission intensity increases as triplet states are converted to singlet states. Clearly the population differences depend on many factors which will be discussed later (see §5), but in exceptional cases the luminescence intensity can be increased by up to five times with microwaves. In summary, the two examples show that one can expect either intensity changes of opposite signs for the circularly polarized emission components in the case of thermalized energy levels or total intensity changes in the case of unthermalized levels where the population differences are principally determined by the emission rates.

The information available from a magnetic resonance spectrum depends on the type of system being investigated but, in general, the analysis of such spectra will be the same for both E.P.R. and O.D.M.R. though in the latter case the line widths tend to be broader and so the determination of the resonance parameters may be more difficult than for E.P.R. The principal part of the magnetic field splitting is described by the g-factor and the simplest resonance condition for an isotropic g-value can be written $h\nu = g\mu_B B$, where $h\nu$ is the microwave energy, μ_B is the Bohr magneton and B is the magnetic field. However, in general, several parameters are needed to describe a magnetic resonance spectrum. The splitting of the levels may be anisotropic if the impurity or defect centre does not have cubic symmetry and so a g-tensor and crystal field parameters would be needed to describe the change in the resonance spectrum as the magnetic field is rotated with respect to the crystal-axes. If there is nuclear interaction within the centre or with neighbours surrounding the centre, then magnetic hyperfine parameters are needed to describe the extra lines observed in the resonance spectrum. Since these latter nuclear interactions are characteristic of the ion involved, it is often possible to identify in considerable detail the nature and structure of the defect in the crystal. Thus, there are many problems where deep centres, i.e. centres where the electrons are tightly bound to the impurity, can be characterized in considerable detail. In contrast to these problems there is another group of defects where generally little or no information can be obtained because the electronic states are determined by the band structure of the crystal. For example, free electrons and holes, bound carriers at shallow donors and acceptors and both free and bound excitons have magnetic properties which are characteristic of the delocalized nature of the states describing these systems. In particular, conduction electron states for cubic crystals where the states are s-like split in a magnetic field with energy proportional to the conduction band g-factor, written as g^* or g_e. This g-factor differs considerably from the Landau value of 2 because of mixing between conduction band states and the valence band states. The hamiltonian describing the magnetic properties of an electron or hole complex has been given by Luttinger [28]

and discussed, for example, by Yafet and Thomas [29] and Zeiger and Pratt [30]. We note, however, that in the case of electrons bound at deep donors and holes bound at deep acceptors, the character of the donors and acceptors is often apparent in the magnetic resonance spectrum. For example, the Ga and In donors in ZnS can be identified and the vacancy and vacancy-associated centres such as V_{Zn}- and (V_{Zn}–Cl) which behave as deep acceptors in donor–acceptor recombination processes, have resonance spectra which can be analysed to determine the nature of the acceptor. See the discussion on ZnS, ZnO and ZnSe in §5.3.

Since the information available from a magnetic resonance spectrum is, in principle, the same for both conventional E.P.R. and O.D.M.R. it is worth considering briefly the advantages of the optical technique. Perhaps the most important is sensitivity since this factor allows an investigation of nominally undoped semiconductors. The extra sensitivity comes about because the weakly allowed magnetic dipole transitions which occur at resonance induce changes in the highly allowed electric dipole transitions of the emission process. An increase of up to 10^5 in sensitivity over conventional E.P.R. could be expected [3] but in practice a factor of 10^3 is probably more realistic, though so far no attempts have been made to calibrate O.D.M.R. spectrometers. Related to the question of sensitivity is the problem in conventional E.P.R. of signal saturation at low temperatures since then no signal can be observed. However, in the O.D.M.R. case saturation produces the maximum change in the luminescence and so is an advantage, though rarely achieved in practice because of inhomogeneously broadened lines (see §3). Another important advantage is the possibility of directly linking a resonance with a particular emission process. Thus, if a resonance line has been identified as belonging to a particular centre, a measurement of the strength of this resonance as a function of luminescence wavelength gives a spectral dependence of the resonance which identifies the emission band associated with the centre. Such a measurement is particularly important where there are several overlapping emission bands and the resonance is related to only one of the emissions. One further point to note is that in conventional E.P.R. it is usual to observe only an absorption of power while in the O.D.M.R. experiment both increases and decreases of the total emission or the circularly polarized emission components can be observed. These changes in the optical case can be interpreted in terms of spin-dependent formation and decay processes and in the case of a decrease in the total emission the observation of centres responsible for non-radiative decay processes is possible.

Before these techniques and the results obtained from the various investigations are discussed in detail it should be noted that only optical magnetic resonance studies involving the detection of microwave induced changes in the luminescence will be discussed. The detection of the ground state by microwave induced changes in the absorption is an important technique (Kemp *et al.* [31]) and so far has not been used to any large extent in semiconductors, though the availability of tunable dye lasers pumped with high-powered krypton ion lasers should enable this technique to be exploited in the future. In particular, the technique is important for linking known E.P.R. signals with unidentified absorption lines or bands—for example, in the case of transition metal ions in semiconductors. Other optical techniques which have been used to study donor states in CdS are the detection of resonance via spin–flip Raman scattered light by Romestain *et al.* [32] and via Faraday rotation by Romestain [33].

Since the recombination and carrier scattering processes in a semiconductor determine the carrier lifetime and electrical properties of a sample it is not surprising to note that the conductivity, photoconductivity, Hall effect and photovoltaic effect can show spin-dependent properties. A discussion of these effects is also outside the scope of this review and the reader is referred to a selection of papers on these effects [21, 34–40] and to a review on the characterization of semiconductors by spin effects to be published by the author [41].

This review deals mainly with recent O.D.M.R. results but in order to emphasize the importance of spin memory effects in semiconductors the following section briefly describes the principles of optical pumping. Section 3 then covers the experimental aspects of O.D.M.R. measurements in preparation for the examples of recombination processes given in §§4–7. Studies of triplet exciton resonances in layered semiconductors described in §4 parallel the many investigations (see Henderson [4]) in insulators and organic materials, though only in the semiconductor does one observe electron and hole resonances. The majority of studies of donor–acceptor pair recombination processes by O.D.M.R. have been in II–VI compound crystals and so §5 summarizes the many results obtained in these materials. Recombination at deep traps is currently of interest since these traps can control the optical and transport properties of semiconductors. The identification of these traps and understanding of the role they play either as radiative or non-radiative centres in the semiconductor processes is of the highest priority and some of the first results obtained by O.D.M.R. are given in §6. Perhaps equally important for new devices is the understanding of recombination in amorphous semiconductors. Some progress has been made in the cases of amorphous (and crystalline) As_2Se_3 and amorphous Si as shown in §7.

§2. Optical pumping in semiconductors

The various aspects of optical pumping in semiconductors have been reviewed in detail by Zakharchenya [5–7], Lampel [8], Planel [9] and Hermann [42]. Only a brief introduction to the application of optical pumping to the investigation of electron g-values will be discussed here and the above references should be consulted for more details of these experiments and, in particular, of the nuclear polarization studies.

Figure 2 illustrates optical pumping in III–V single crystals with tetrahedral symmetry. The conduction band is Γ_6 with $S=\frac{1}{2}$ and is isotropic whereas the valence band is split by spin–orbit interaction, energy Δ, into two bands, Γ_8 and Γ_7 with $J=\frac{3}{2}$ and $J=\frac{1}{2}$ respectively. In these materials Δ is of the order of the band gap energy, E_g. The figure shows the allowed transitions for excitation of the crystal with $\sigma+$ radiation and it can be seen that if the excitation energy is resonant with the band gap only the transitions $|-\frac{3}{2}\rangle \rightarrow |-\frac{1}{2}\rangle$ and $|-\frac{1}{2}\rangle \rightarrow |+\frac{1}{2}\rangle$ occur. Since the transition strengths are unequal the $|-\frac{1}{2}\rangle$ electron–spin state is more populated than the $|+\frac{1}{2}\rangle$ spin state. The electron polarization was defined in eq. (1.1) and for optical pumping in III–V compound crystals we see that $P=-0{\cdot}5$. This initial polarization of the electron spins will be modified depending on the degree of thermalization, if any, before emission. Thus, the spin polarization at the instant of emission will be

$$P=-0{\cdot}5\frac{T_1}{T_1+\tau}, \tag{2.1}$$

where T_1 is the spin lattice relaxation time and τ is the optical lifetime. Assuming the

Fig. 2

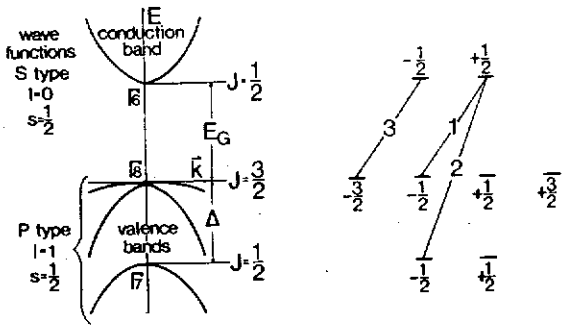

Optical pumping in a zinc blende crystal showing the excitation transitions for σ^+ radiation. For energy $\sim E_g$ only the $-\frac{3}{2}\rightarrow\frac{1}{2}$ and $-\frac{1}{2}\rightarrow+\frac{1}{2}$ absorption occurs. (After Weisbuch and Hermann [45].)

same transition rates in emission the degree of polarization of the emission will be

$$\theta=\frac{I_{\sigma+}-I_{\sigma-}}{I_{\sigma+}+I_{\sigma-}}, \tag{2.2}$$

$$=0{\cdot}25\frac{T_1}{T_1+\tau}. \tag{2.3}$$

Therefore, if the spin memory is complete (i.e. $T_1 \gg \tau$) an emission polarization of 25% would be observed. Parsons [43] was the first to observe the effect of optical pumping on the degree of circular polarization of the emission in GaSb single crystals. Excitation near the band gap with circularly polarized light produced an emission polarization of 23% in excellent agreement with the expected results. Note that this polarization is produced in *zero* magnetic field.

Since the emission polarization depends on the electron-spin polarization, magnetic resonance of the conduction electrons can be detected by monitoring the degree of emission polarization. The experiment is carried out in the presence of a magnetic field set parallel to the direction of emission and transitions between the two spin states are induced by radio frequency radiation giving a reduction of the spin polarization which in turn decreases the emission polarization. The first successful measurement of a conduction electron g-value by optical pumping was carried out by Hermann and Lampel [44] who investigated p-type GaSb. Monochromatic circularly polarized light with energy of 0·813 eV was focused onto the sample at 2 K and luminescence of the I_1 line at 0·777 eV was monitored with a circular polarizer and PbS cell. Resonance corresponding to $|g_e|=9{\cdot}3\pm0{\cdot}3$ was induced by an r.f. field at 150 MHz and detected as a derivative signal using field modulation. The success of the technique showed the way to investigate electron g-values in undoped semiconductors.

An apparatus for investigating optical pumping and resonance in semiconductors is shown in fig. 3 from the work of Weisbuch and Hermann [45]. The sample is immersed in liquid helium at 2 K and luminescence is excited by a laser resonant with

the band gap energy. In order to measure the degree of spin memory the excitation radiation is linearly polarized and modulated between σ^+ and σ^- with a stress plate modulator at 50 kHz. Circularly polarized luminescence is detected by a photomultiplier and lock-in detector operating at the excitation modulating frequency. The figure also shows an r.f. coil and a longitudinal magnetic field used for the magnetic resonance experiments. In order to illustrate the optical pumping technique results of an investigation of CdTe by Cavenett *et al.* [46] and Nakamura *et al.* [47] will be discussed. The emission of high purity CdTe crystals excited by band gap radiation from a dye laser is shown in fig. 4. The most intense line is due to the recombination of excitons at neutral acceptors labelled (A^0, X). Free excitons with $n=1$ are labelled by X and excitons recombining at neutral and ionized donors are labelled (D^0, X) and (D^+, X) respectively. The polarization of the emission was measured as described above and is shown in fig. 5. The maximum polarization was observed on (A^0, X). In order to determine the feasibility of a resonance experiment the Hanle effect is measured by applying a magnetic field transverse to the direction of emission. The spin magnetization created in zero magnetic field by the circularly polarized pump light is rotated away from the emission direction by the transverse field. The emission polarization decay is lorentzian with a half width

$$\Delta B_x = \frac{h}{|g_e|\mu_B}\left[\frac{1}{T_2}+\frac{1}{\tau}\right], \tag{2.4}$$

where T_2 is the transverse relaxation time. For zero longitudinal magnetic field $T_1 = T_2$ and so measurements of polarization, θ, and the Hanle width allows the determination of T_1 and τ. The value of the transverse field, B_x, required to quench the polarization is an indication of the magnitude of the oscillatory B_x needed in the resonance experiment. Figure 6 shows the Hanle curve for the (A^0, X) emission of CdTe where ΔB_x of 10 G indicates that approximately 50 W of r.f. power is required

Fig. 3

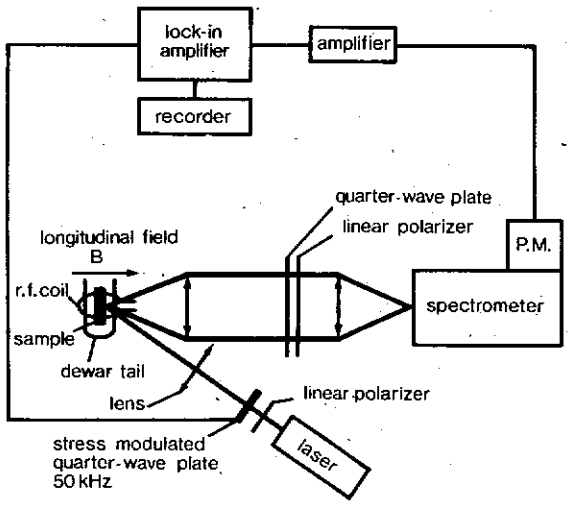

Experimental arrangement for optical pumping and magnetic resonance in semiconductors. (After Weisbuch and Hermann [45].)

Fig. 4

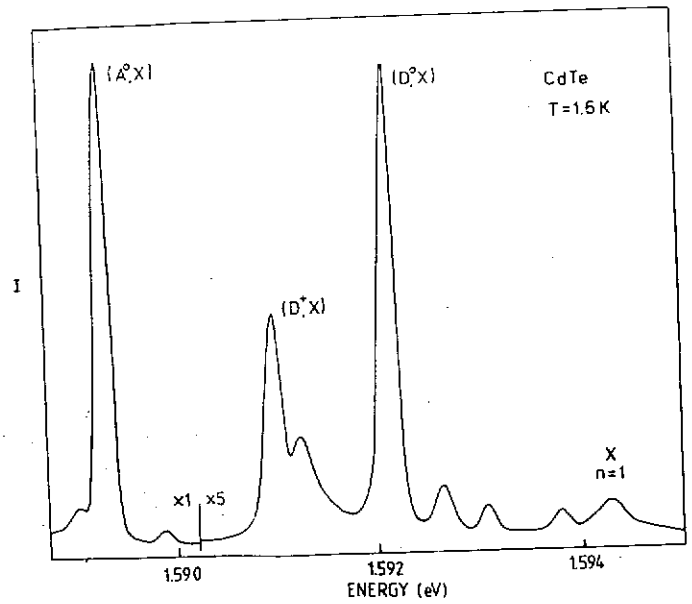

Emission spectrum for CdTe at 1·7 K excited with 800 nm radiation from a dye laser.

Fig. 5

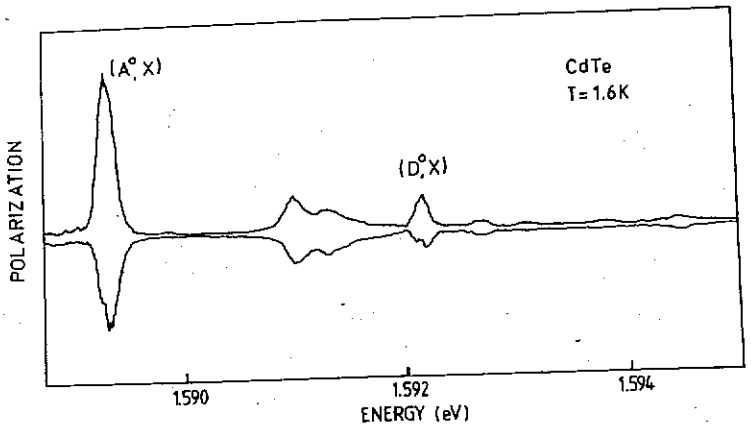

Emission polarization spectra for CdTe measured with apparatus shown in fig. 3.

for the C.E.S.R. experiment. The conduction electron resonance is shown in fig. 7 for 151 MHz. The emission polarization decreased 30% at a magnetic field corresponding to a value of $g_e = 1{\cdot}59 \pm 0{\cdot}02$ where the sign was determined by observing the magnetic field shift of the C.E.S.R. line when the Cd and Te nuclei were polarized by using unmodulated excitation light as discussed by Weisbuch [48]. The reason for the investigation was the uncertainty of the value of g_e because of the many different reported values. A value of $-1{\cdot}1 \pm 0{\cdot}1$ had been deduced from N.M.R. measurements

Fig. 6

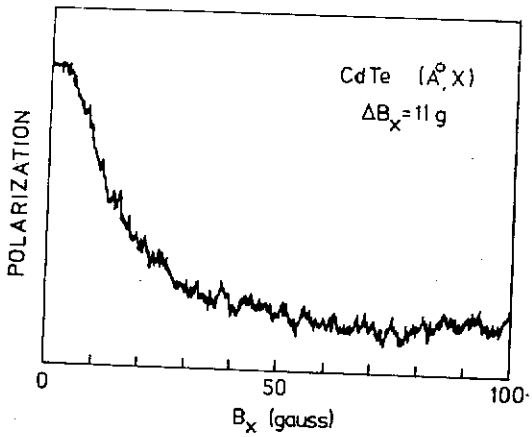

Hanle curve for (A^0, X) emission in CdTe.

Fig. 7

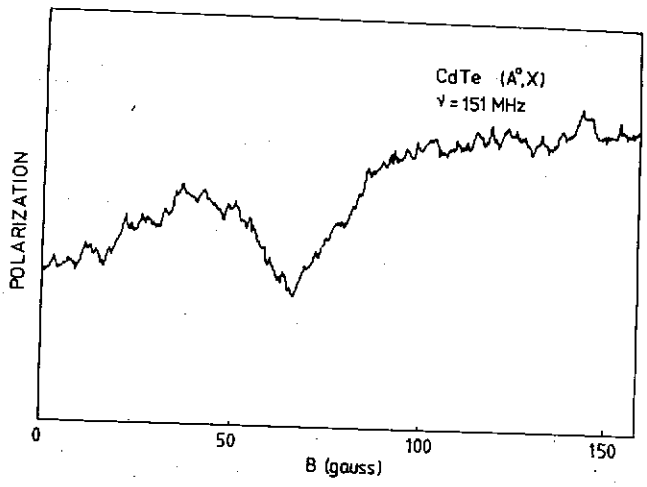

Electron resonance observed as a decrease in the emission polarization at 151 MHz.

by Look and Moore [49], −0·74 had been obtained from splin–flip Raman measurements by Walker *et al.* [50] and conventional E.S.R. on doped CdTe gave a value of $1{\cdot}6803 \pm 0{\cdot}0005$ by Alekseeno and Veinger [51]. The C.E.S.R. measurement agrees with the conventional E.S.R. measurement since in doped material the donor g-value is commonly larger than the value for pure crystals (see §5 for results on ZnSe by Dunstan *et al.* [52]).

The importance of the C.E.S.R. experiments for determining the electron g-values which provide a detailed test of band structure calculations has been shown in the two papers by Weisbuch and Hermann [45] and Hermann and Weisbuch [53] who investigated both by experiment and theory the variation of g-value in III–V compound alloy crystals. An example of their experimental results is shown in fig. 8 where it can be seen that the addition of Al to GaAs decreases the electron g-value

Fig. 8

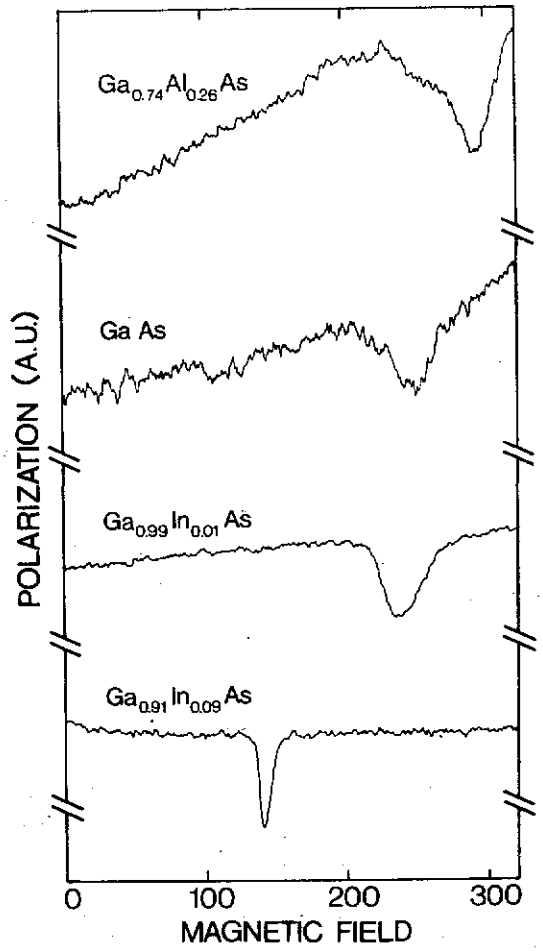

Electron resonances observed in GaAs and alloy semiconductors $Ga_xAl_{1-x}As$ and $Ga_xIn_{1-x}As$ showing the change in g-value. (After Weisbuch and Hermann [45].)

while the alloying of In increases g_e. A comparison of the effective masses m^* and the g-factors with predictions of the k.p. theory provided values for the interband coupling parameters for the III–V and II–VI semiconductors. In particular, there was excellent agreement with the measured values of g_e for the alloys $Ga_{1-x}In_xAs$ and $Ga_{1-x}Al_xAs$.

The authors were able to predict a value of between $-0{\cdot}1$ and $+0{\cdot}3$ for g_e in ZnTe suggesting that the value of 1·74 measured by spin–flip Raman was not due to conduction electrons. This prediction has been shown as good by recent magneto-optical and O.D.M.R. measurements which are discussed in §5.

§3. Optically detected magnetic resonance measurements

In the case of the O.D.M.R. experiments the way in which the sample is excited with the laser is generally less important than in the optical pumping experiments

where the excited state population differences are created by the pump light. There is no need, for example, to excite the crystal with near band gap radiation. In fact, the choice whether to use radiation which has energy greater or less than the band gap depends on the problem involved. For example, in the cases of bulk excitation of defects in direct gap semiconductors such as ZnSe and GaAs light with energy less than the band gap would be preferable while in the case of defects in implanted layers or epitaxial layers, band gap radiation restricts the studies to these layers. It must be remembered, however, that these comments must be taken as general guidelines and observation of O.D.M.R. and enhancement of the signals by optical pumping may depend critically on the choice of energy, intensity or polarization of the excitation radiation.

Many O.D.M.R. experiments can be carried out by using a conventional magnet spectrometer similar to that described by Geschwind [3]. In general such a system will use a cylindrical cavity similar to the one illustrated in fig. 9 (*a*). The sample is excited by a laser beam which passes through a hole in the bottom of the cavity and the luminescence is collected through the horizontal grids in the wall of the cavity. The X-band cavity illustrated in the figure has a TE_{012} mode and is quartz filled to reduce the size. This cavity and excitation configuration is very suitable when defects and impurities in semiconductors are being investigated with laser radiation energy less than the band gap. However, where band gap excitation is necessary it is usual to observe the luminescence from the surface of the crystal being illuminated by the laser. The rectangular X-band cavity shown in fig. 9 (*b*) has proved to be very successful when used with a split coil superconducting magnet. The sample is mounted on the removable grid at the end of the cavity and the luminescence can be very efficiently collected in a direction parallel to the magnetic field allowing the circular polarization properties of the luminescence to be investigated. Clearly, the front face illumination is important for studies of epitaxial layers. (See § 6.)

An O.D.M.R. system using a superconducting magnet of 2·5 T with rectangular cavities at 9 GHz and 17 GHz as described above is shown in fig. 10. The sample,

Fig. 9

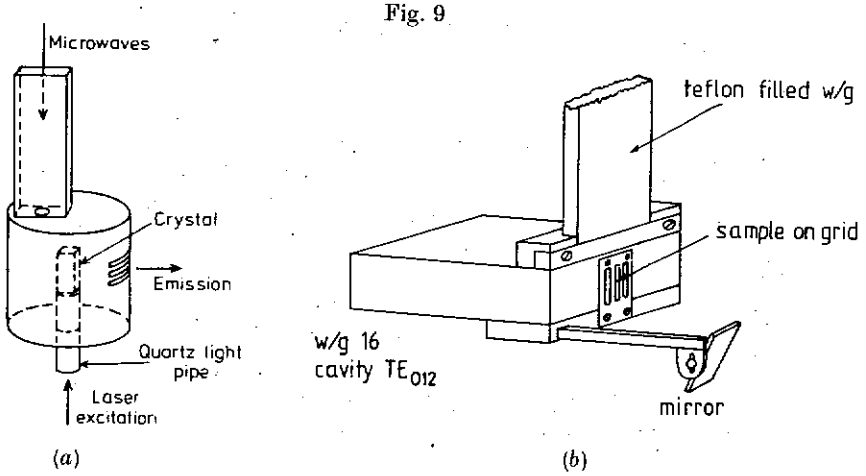

(*a*) Diagram of quartz filled TE_{012} cavity showing excitation through quartz light pipe sample holder and emission through slots in the cavity wall. (*b*) Rectangular TE_{012} cavity for front face illumination showing mirror for laser excitation and grid in sample holder for monitoring emission.

Fig. 10

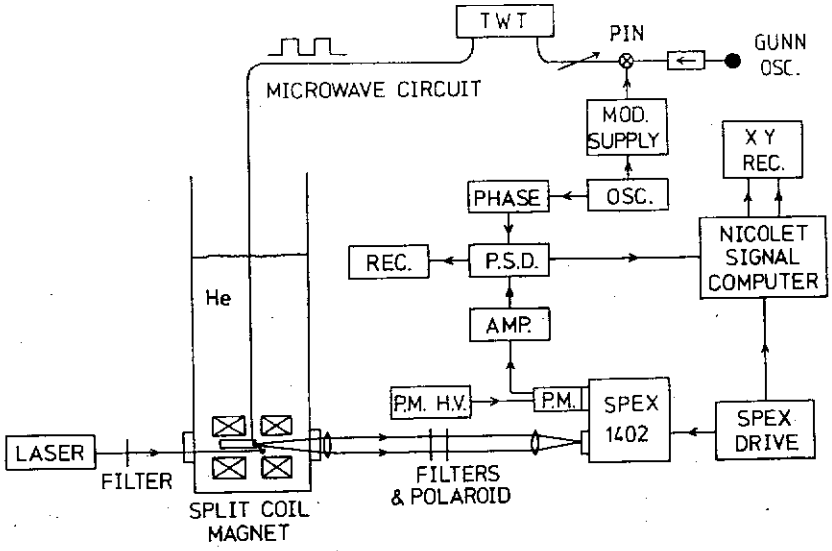

Experimental arrangement of O.D.M.R. spectrometer using a superconducting magnet.

cavity and magnet are all immersed in liquid helium at 2 K. Luminescence from the sample is excited by an argon, krypton or Nd : YAG laser radiation and the emission is monitored by a photomultiplier or infrared-detector in a direction parallel to the magnetic field so that microwave induced changes in either the total intensity or one of the circularly polarized components can be detected. For the visible region Polaroid circular polarizer is used to analyse the emission while in the infrared a linear polarizer can be used with a Fresnel rhomb or mica $\lambda/4$ plates. Microwave power is provided by a combination of a klystron or Gunn oscillator and a travelling wave tube amplifier. The microwaves are switched at audio frequencies either by modulating the reflector voltage or by using a lock-in detector operating at the microwave chopping frequency. A signal averager is often necessary to enhance the signal-to-noise. The sign of the emission change is measured by comparing the wave form of the chopped microwaves with the waveform of the signal taken directly from the photomultiplier and accumulated on the signal averager. Also, by recording with a single scan the magnitude of the d.c. voltage from the photomultiplier and comparing it with the accumulated a.c. voltage, the magnitude of the optical resonance signal can be obtained from $V_{\text{a.c.}}/V_{\text{d.c.}}=\Delta I/nI$ where n is the number of signal averager scans needed to accumulate the a.c. voltage.

It is useful to note that the microwave circuit is much less critical for O.D.M.R. than for E.P.R. and, for example, an A.F.C. system for the microwave oscillator, although desirable, is not necessary, particularly at X-band where very stable oscillators are available. The choice of microwave frequency is also less important for O.D.M.R. than E.P.R. because in the case of the unthermalized systems there is no signal-to-noise advantage gained by carrying out experiments at frequencies above 9·5 GHz. In the case of thermalized systems and for higher resolution the use of a millimetre spectrometer is of advantage. Since travelling wave tube microwave amplifiers with greater than 10 W are available with 8–18 GHz frequency range the author has found that a dual frequency system (WG16 and WG18) with a

superconducting magnet is a useful spectrometer. Spectrometers at 23 GHz (K-band) and 35 GHz (Q-band) using cylindrical cavities are also important for high resolution, though limited for some problems by the availability of high-powered klystrons (maximum after PIN switch ~300–500 mW). The most commonly used chopping frequencies are 100 HZ–5 kHz since at lower frequencies the $1/f$ noise becomes intolerable and, in many cases, the signals reduce in magnitude above 5 kHz. Even within this narrow frequency range the choice of chopping frequency can be important with some signals best observed at low frequencies (e.g. A-centre in ZnS and narrow electron resonances in a-Si : H) and other resonances more intense or only observed at higher frequencies (acceptor resonance in a-Si : H, O^- centre in GaP). The intensity of the laser power excitation can often be equally important since in some cases the signal strength increases with decreasing laser power (see § 4) for GaSe and [54]). Similarly, the microwave power level can also be important and although high powers have been considered essential, the observation of cyclotron resonances via the electron–hole drop emission in germanium can only be carried out at very low powers [55], and recent measurements at 35 GHz have also been at low power [184].

Two methods of enhancing the O.D.M.R. signals are used routinely. One has been mentioned above and is the use of circularly polarized pump light to enhance the population differences between the Zeeman levels of partially thermalized systems. Such an enhancement is shown in fig. 11 for the case of GaAs : Cr O.D.M.R signals from the 0·839 eV emission where an increase of more than a factor of 10 is observed

Fig. 11

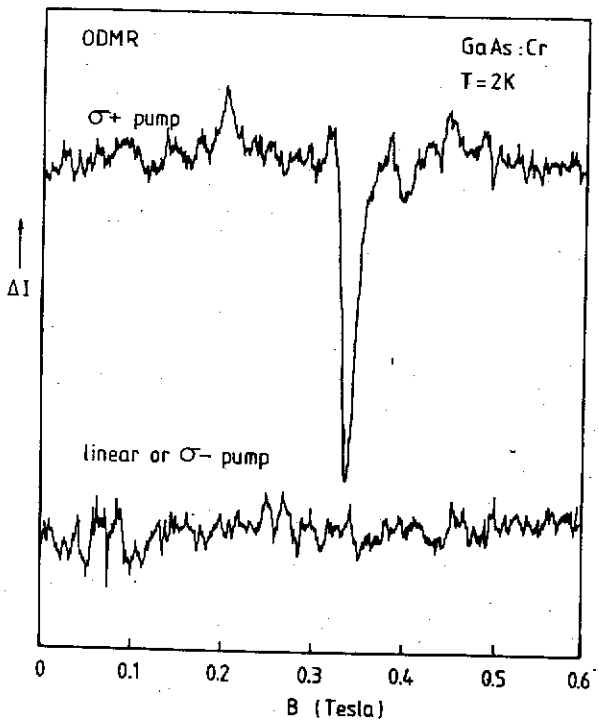

Illustration of the enhancement of O.D.M.R. signals by optical pumping. Upper curve is the GaAs : Cr signal exciting with σ^+ polarized light while lower curve has been obtained by pumping with linear or σ^- radiation.

with circularly polarized pump radiation (see §6). Similar enhancements have been observed for excitons in GaSe (see §4). The second enhancement method is the field modulation technique which was first used by Schnegg *et al.* [56] and more recently investigated by Davies [57] and Manson and Edgar [58]. The method involves modulating the magnetic field with an a.c. field. This field sweeps the resonance through the spin packets of an inhomogeneously broadened line and enhancements of greater than a factor of 10 can be obtained for some systems. An example from the work of Davies [57] is shown in fig. 12 for the donor and acceptor resonances in ZnSe : F.

One of the most important measurements in an O.D.M.R. experiment is to determine which of the emission lines or bands change in intensity at resonance. These so-called spectral dependence measurements are carried out by replacing the filters from in front of the photomultiplier by a spectrometer and then setting the magnetic field to resonance and scanning through the luminescence in order to record the emission change, ΔI, as a function of wavelength. This measurement is complicated when non-resonant signals (or background signals) are present and since most semiconducting samples show such signals which are generally proportional to the emission intensity some caution must be exercised in determining which emission band is producing the resonance signal or signals. One technique is to record the spectral dependence at two magnetic fields, on and off resonance, and subtracting the two curves to give the required result. In cases when there are several resonances and many emission lines, it is more satisfactory to record the resonances by scanning the magnetic field for each emission line. Another method can be used when the resonances can be enhanced by applying an oscillating longitudinal field as discussed above. Since the non-resonance signals are not affected by the modulation Davies [57] has shown that by chopping the enhancement modulation with continuous

Fig. 12

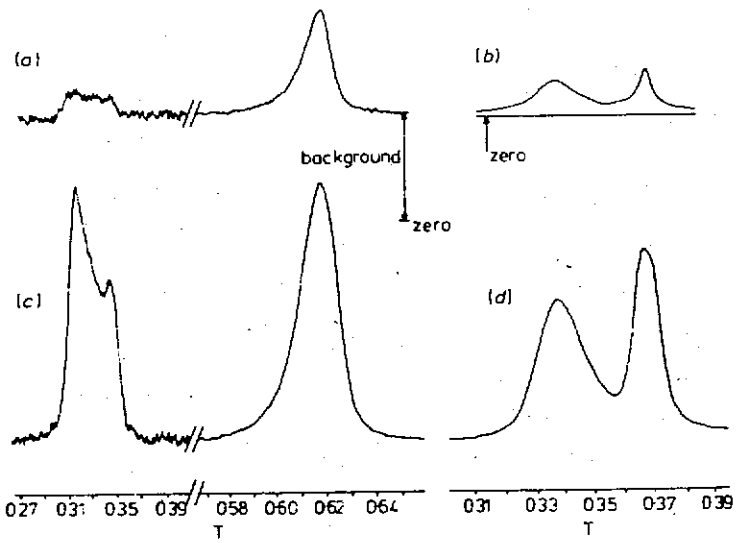

Examples of enhancement of O.D.M.R. signals by application of 100 kHz modulation to the main magnetic field. (*a*) ZnSe : F and (*b*) ZnS : Al are signals without enhancement while (*c*) and (*d*) show the increased S/N with the modulation. (After Davies [57].)

microwaves and detecting at this frequency the background signal is reduced by ~200. Clearly, field modulation techniques as used for conventional E.P.R. to give derivative resonance signals should remove the background signal but, in general, the field modulation gives weaker signals than the amplitude modulation of the microwaves. In fact, often no signal can be observed by the field modulation method. Undoubtedly, the very broad lines often observed in O.D.M.R. make the field modulation method less satisfactory particularly when it must be remembered that the modulation detection frequency is usually very much less than the convenient 100 kHz of conventional E.P.R. (However, see §8.)

§4. Exciton resonances in GaSe and GaS

GaSe and GaS are III–VI semiconductors with layered structures where the building blocks are four-fold planar layers held together by covalent bonds as shown in fig. 13. The solid circles are Ga atoms and the open circles are Se or S atoms; it can be seen that the structure is characterized by the Ga—Ga bonds. The crystals are formed by stacking these layers one on top of the other where the layers are held together by weak van der Waals' forces. Since the layers can be stacked with different sequences the crystals can exhibit different polytypes as shown in fig. 14 for the three well-known types: hexagonal β and ε, and rhombohedral γ. A fourth polytype, hexagonal δ, has been more recently reported by Kuhn *et al.* [59]. In general, GaSe crystals are either ε or γ polytypes or mixtures of the two whereas crystals of GaS usually have the β-stacking. Details of optical and electrical properties of these crystals can be found in the review by Mercier *et al.* [60] and, in particular, the luminescence properties have been summarized by Voitchovsky and Mercier [61]. In fact, these latter authors have shown that the luminescence spectra of GaSe crystals can be described in terms of two spectra, one corresponding to that observed in lightly doped crystals and designated the $A(h\nu)$ spectrum and the other corresponding to heavily doped crystals and called $C(h\nu)$. Typical emission spectra

Fig. 13

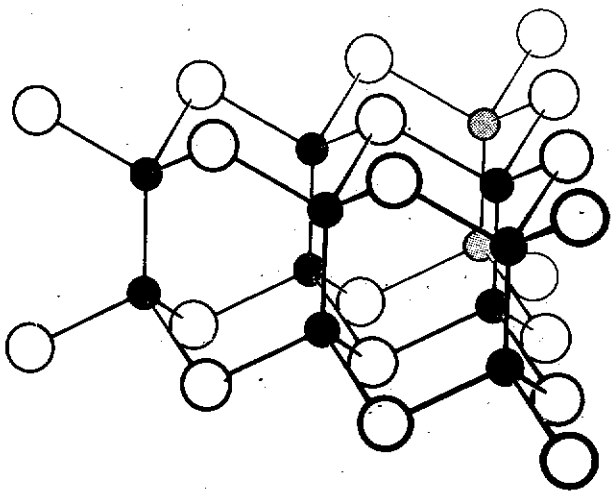

Crystal structure of GaSe showing the layers of Se (○) and Ga (●) atoms and the Ga–Ga bonds. (After Mercier *et al.* [60].)

Fig. 14

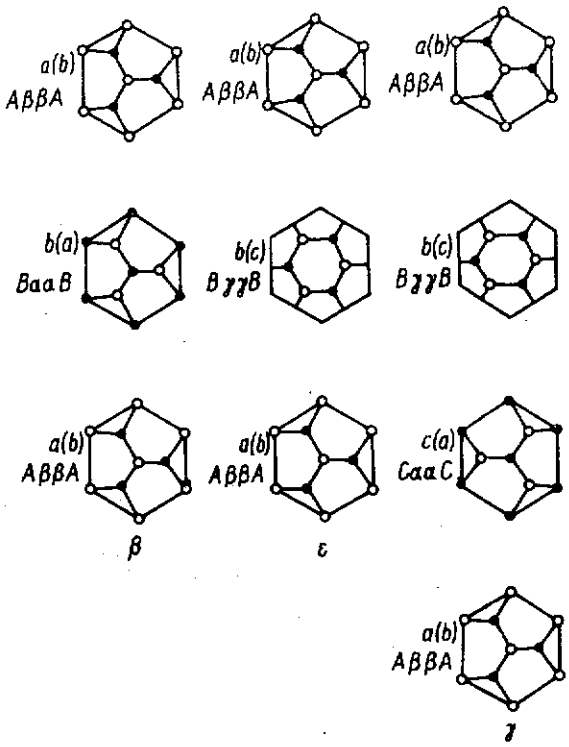

Illustration of the principal polytypes α, β and γ in GaSe. (After Abdullaeva and Mamedov [192].)

from two types of GaSe crystals are shown in figs. 15 and 16 where it can be seen that in some samples a strong free exciton line and many well-resolved bound exciton lines are observed while in other samples (fig. 16) the free exciton is very weak ($\sim$ 1/200 of bound exciton emission) and the bound excitons are poorly resolved.

The origin of the various sharp and broad emissions in GaSe has been controversial for many years and, in particular, the work by Voitchovsky and Mercier [61] and Mercier *et al.* [60] favoured a donor–acceptor-model for these emissions. Kuroda and Nishina [62], however, interpreted these emissions as arising from the recombination of bound excitons associated with the indirect gap. The controversy was resolved by the optical magnetic resonance studies by Dawson *et al.* [63], Morigaki *et al.* [64], Cavenett *et al.* [65] and Dawson *et al.* [66] who observed triplet exciton resonances from all of the sharp lines except the free exciton emission.

The optical magnetic resonance studies were carried out on a variety of GaSe crystals supplied by Kuroda and Nishina of Sendai University and Levy of École Polytechnique, Lausanne. The crystals cleaved easily giving surfaces perpendicular to the c-axis and the emission was monitored in a direction parallel to the c-axis and the magnetic field. In the case of crystals showing the emission given in fig. 15 the resonances shown in fig. 17 were observed for the two polarizations, σ^+ and σ^-. The triplet exciton resonances which corresponded to changes in the polarized emission components of approximately 0·1% could be seen at 0·22 T and 0·48 T and were observed by monitoring the 592–600 nm emissions. The electron resonance observed

Fig. 15

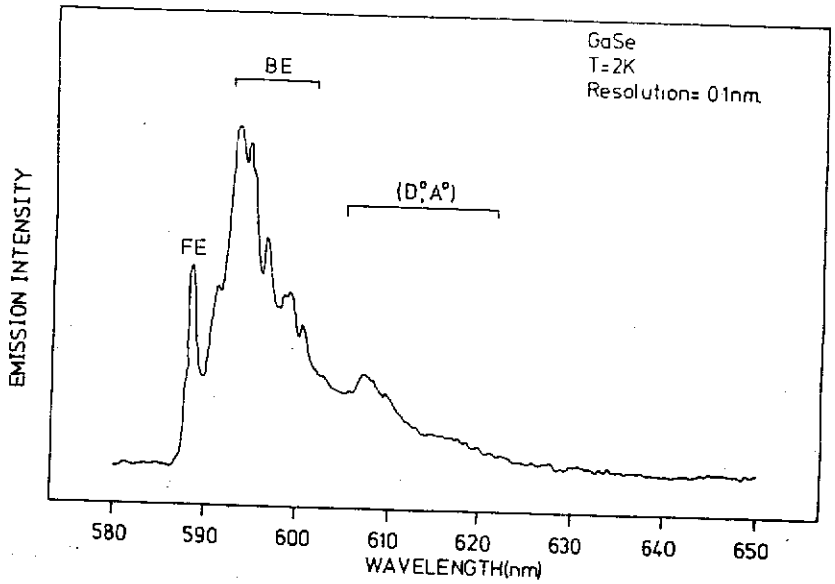

Emission spectrum for type I GaSe showing the intense free exciton emission at 588 nm and the bound exciton emissions.

Fig. 16

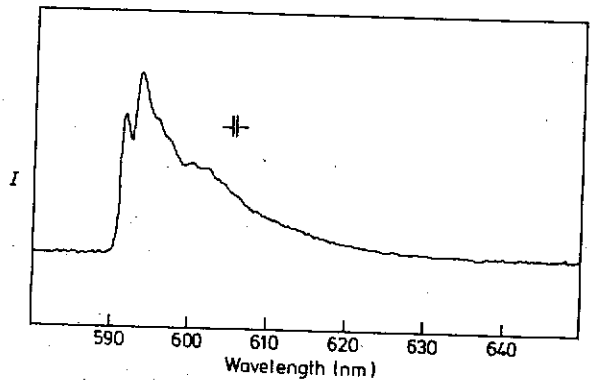

Emission spectrum for type II GaSe.

at high field with $g_{e\parallel} = 1{\cdot}13 \pm 0{\cdot}01$ was observed from the 588–617 nm emissions which includes the free exciton, bound exciton and donor–acceptor transitions. The hole resonance with $g_{h\parallel} = 1{\cdot}72 \pm 0{\cdot}02$ was observed by monitoring all of the emissions except the 617 nm band. No exciton resonance was observed on the free exciton emission at 588 nm but at 590 nm a triplet exciton resonance at slightly different field values from fig. 17 was observed in some crystals. The exciton resonances have been interpreted in terms of an unthermalized triplet ($S = 1$) energy level scheme based on the spin-hamiltonian

$$\mathscr{H} = g_{ex\parallel}\mu_B B_z S_z + g_{ex\perp}\mu_B[B_x S_x + B_y S_y] + D[S_z^2 - \tfrac{1}{3}S + 1)], \qquad (4.1)$$

Fig. 17

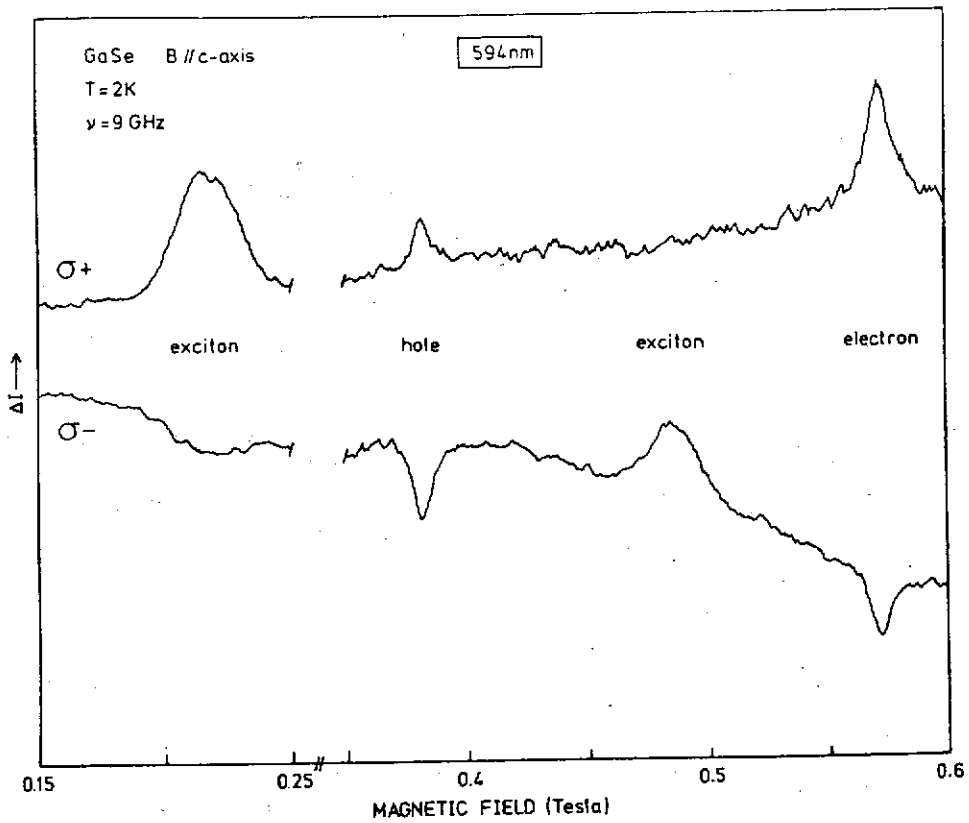

O.D.M.R. signals for the 594 nm bound exciton emission in GaSe (type I) with $B \| c$-axis showing the exciton, hole and electron resonances.

where the c-axis of the crystal is taken as the z-axis and $g_{ex\|} = 1{\cdot}85 \pm 0{\cdot}03$ and $D = +0{\cdot}110 \pm 0{\cdot}004\,\mathrm{cm}^{-1}$. The microwave resonances are shown in fig. 18 as transitions $|0\rangle \rightarrow |+1\rangle$ at low magnetic field and $|0\rangle \rightarrow |-1\rangle$ at high field. These occur because the population differences are established in an unthermalized system by the relative decay rates from the three states. For $B \| c$-axis the allowed radiative transitions are shown in the figure and the populations of the $|\pm 1\rangle$ states fall below the $|0\rangle$ state. Thus at the exciton resonances either the σ^+ or σ^- emission increases; fig. 17 shows that the low field resonance can also be seen as a decrease of the σ^- emission and this has been attributed to some degree of thermalization between the $|0\rangle$ and $|-1\rangle$ states.

In order to confirm the triplet nature of the excitons the circular polarization of the emission, $[I_{\sigma-} - I_{\sigma+}]$ was measured as a function of magnetic field. As can be seen from fig. 18, a level crossing of the $|0\rangle$ and $|-1\rangle$ states occurs at $0{\cdot}13\,t$ and at this value an increase of the $\sigma-$ emission would be expected. This was observed as shown in fig. 19. The level crossing corresponding to the resonances in fig. 17 is labelled by the emission wavelength 594 nm. It is noted that the 590 nm level crossing occurs at 0·164 T, a value 0·014 T larger than that for the 594 nm emission. This is consistent with the observation of a slightly larger zero field splitting for excitons associated

Fig. 18

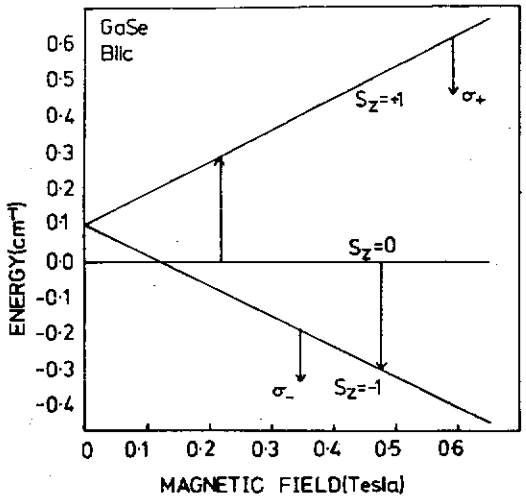

Energy level scheme for unthermalized triplet excitons in GaSe with $B \| c$-axis.

Fig. 19

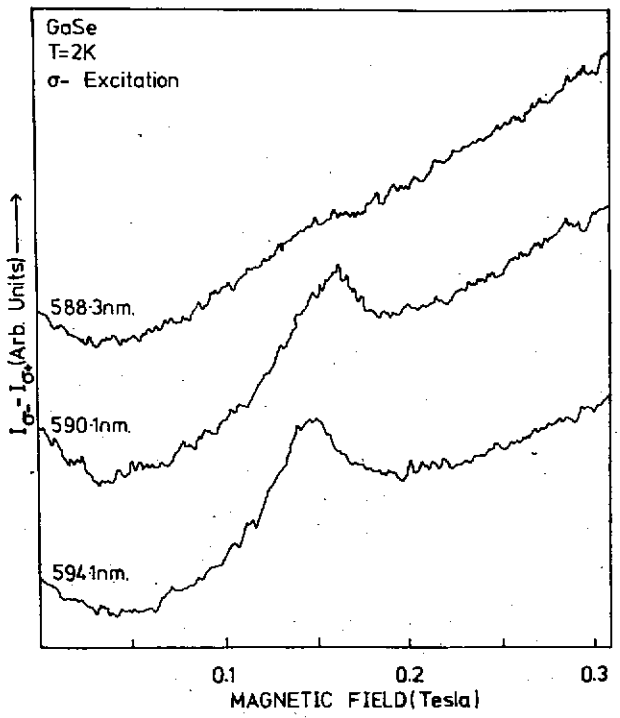

Magnetic circular polarization measurements for the free excitons (588 nm), bound excitons associated with the direct gap (590 nm) and bound excitons associated with the indirect gap (594 nm). The crossing of the -1 and 0 levels increases the σ^- emission intensity. (See fig. 18.)

with this emission. The level crossing on the 588 nm emission shows optical pumping behaviour very different from the bound excitons and has been attributed to the free excitons.

The assumption that the $g_{e\parallel} = 1{\cdot}13$ and $g_{h\parallel} = 1{\cdot}72$ were due to free electrons and holes was based on the observations that these resonances were observed on the free exciton emission. The line width of the electron resonance $\Delta B_{1/2} \sim 5$ mT was observed to be narrower than the hole resonance, $\Delta B_{1/2} \sim 7$ mT, which is consistent with the general observation that the anisotropy of electron g-values is smaller than for holes and so the electron resonance would be less dependent on crystal imperfections and strains. This assumption is in agreement with magneto-optical absorption measurements by Brebner [67] for the magnetic field perpendicular to the c-axis where $g_{\perp} = 1{\cdot}2$ for both electrons and holes. More recently the confirmation that the high field resonance is due to electrons has been provided by Dawson *et al.* [66] who observed an Overhauser shift of this resonance by pumping with circularly polarized light (see § 2). The degree of nuclear polarization is proportional to the magnitude of the electronic polarization. If unmodulated circularly polarized light is used to excite the luminescence the nuclear polarization produces an internal magnetic field which gives an apparent shift of the resonance as shown in fig. 20 for GaSe. Reversing the sense of polarization, reverses the nuclear magnetic field direction with respect to the external field and so the resonance shifts in the opposite direction as shown. The electron and hole resonances were observed as equal and opposite polarization changes; such an observation implies that the free electrons and holes are thermalized. The results were understood in terms of the model shown

Fig. 20

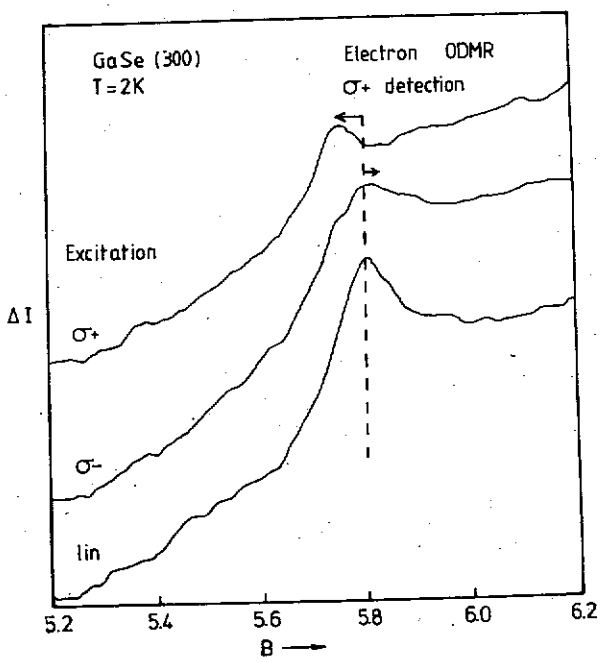

The electron resonance field position depends on the polarization of the pump beam which produces a nuclear polarization and hence an internal magnetic field. Thus the resonance for σ^+ occurs at lower magnetic field than for σ^-.

in fig. 21 where free electrons and holes combine spin dependently to form free excitons. The electron resonance increases the population of the $S_z = +\frac{1}{2}$ level with respect to the thermal equilibrium values so that more free triplet excitons with $S_z = +1$ and less with $S_z = -1$ are created than before resonance. Similarly, the hole resonance increases the σ^+ emission and decreases the σ^- emission.

Before the origin of the triplet resonances is discussed it is important to note that a second triplet resonance can be observed in crystals showing the emission in fig. 16. These crystals were called type II by Cavenett *et al.* [65] and a typical resonance spectrum is shown in the upper part of fig. 22 and the level crossing is shown in the lower part. It can be seen that the zero field splitting (equal to half the separation of the resonances) is much larger. In fact, using the hamiltonian, eqn. (4.1) given above, it was found that these excitons have the same $g_{ex\parallel} = 1{\cdot}87 \pm 0{\cdot}03$ as in the type I crystals but the value of the zero field splitting was $D = +0{\cdot}288 \pm 0{\cdot}002\ \mathrm{cm}^{-1}$ when all light was monitored. When a spectral dependence of the resonances was measured emission line by line using the Spex 1402 monochromator, two slightly different D values were observed. From the 591 nm emission a value $D_1 = +0{\cdot}283 \pm 0{\cdot}004\ \mathrm{cm}^{-1}$ was measured and from the 594 nm line $D_2 = +0{\cdot}288 \pm 0{\cdot}004\ \mathrm{cm}^{-1}$ was determined. Emissions at longer wavelengths were found to be mixtures of these two spectra with the D value dependent on the relative contributions from the phonon side bands of the 592 nm and 594 nm emissions.

The exciton optical resonance results show that the sharp line emissions in GaSe are the result of triplet exciton recombination. The most important questions are 'Where are the excitons localized?' and 'Why are there only two exciton spectra?' but only partial answers can be given to these questions at this stage of the investigation. It is clear that the centre of localization does not contribute a particle (electron or hole) to the exciton complex and so the centre will either be an ionized donor, isoelectronic trap or a structural defect. The isoelectronic trap oxygen is a very likely impurity.

Fig. 21

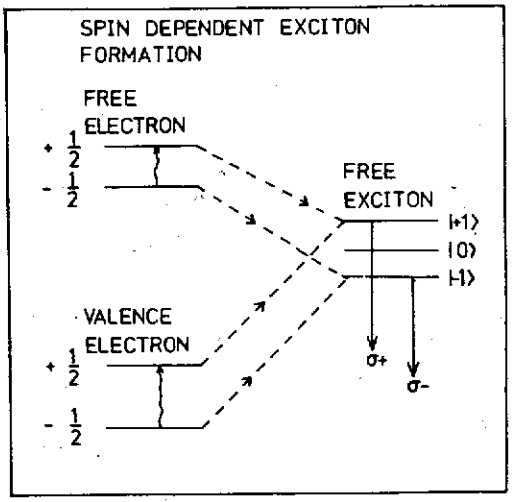

Spin dependent formation of free excitons from free electrons and free holes. Both electron and hole resonances increase σ^+ and decrease σ^-.

Fig. 22

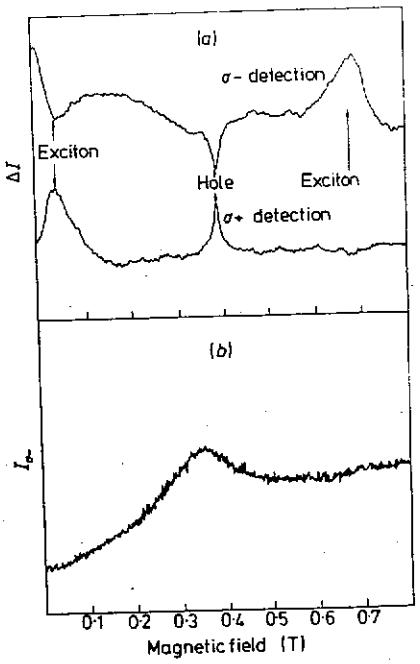

(*a*) O.D.M.R. signals for the type II GaSe showing the broad and strong triplet exciton resonances and the hole resonance. (*b*) Level crossing measurement for $I_{\sigma-}$.

Although small variations of the D value are observed for both type I and type II resonances, there is a clear correlation between the emission spectrum and the type of resonance observed. Basically, where strong FE emission and sharp bound exciton lines are observed the exciton with $D = +0{\cdot}11\ \text{cm}^{-1}$ is observed whereas when no FE is obvious and the sharp lines are less resolved the resonance with $D = +0{\cdot}288$ is detected. Sometimes in the latter type II crystals the type I resonance is observed very weakly but so far the type II resonance has not been seen in type I crystals even though this resonance is very strong and would easily be detected. Cavenett *et al.* [65] suggested that the observation of the two resonance spectra with the same g-value was possibly due to different stacking of the layers in the two types of crystals. The γ and ε polytypes are the most common crystal forms and so one possibility is that similar defects are present in both types of crystals and the D value depends on whether the crystal has γ or ε stacking. The association between the $A(h\nu)$ and $C(h\nu)$ spectra discussed by Mercier *et al.* [60] and the occurrence of the two resonances is not yet clear since the type I emission is a mixture of the A and C spectra but the two resonances are not observed in these crystals. It should be noted that Mercier *et al.* [60] have associated the $C(h\nu)$ or type II spectrum with crystals containing a large number of impurities. The understanding of these results has been further complicated by recent measurements by Dawson *et al.* [66] who have observed a third triplet resonance in GaSe : Cu material. In fact all three triplets are present and a sharp $\Delta M_J = 2$ transition common to all three systems with the same g-value is observed. For this new triplet $D = 0{\cdot}217 \pm 0{\cdot}004\ \text{cm}^{-1}$. A summary of the observed magnetic resonance parameters is given in table I. Clearly a considerable amount of work is necessary to clarify the nature of the localization of the excitons in GaSe. At

Table 1. O.D.M.R. parameters for triplet excitons in GaSe and GaS.

Material	Label	$g_{\parallel}$	$g_{\perp}$	D (cm^{-1})	^{69}Ga A (cm^{-1})	^{71}Ga A (cm^{-1})
GaSe	I	1·85 ± 0·03	—	+0·110 ± 0·004	—	—
g_e = 1·13 (0·01)	II	1·85 ± 0·03	—	+0·288 ± 0·004	—	—
g_h = 1·72 (0·02)	III	1·85 ± 0·03	—	+0·217 ± 0·004	—	—
GaS	I	2·006 ± 0·003	1·87 ± 0·06	+0·013 ± 0·001	—	—
	II	2·006 ± 0·003	—	+0·024 ± 0·001	—	—
	IIIA	2·006 ± 0·003	—	+0·028 ± 0·001	0·018 ± 0·001	0·025 ± 0·001
	IIIB	2·006 ± 0·003	—	+0·028 ± 0·001	0·025 ± 0·001	0·034 ± 0·001
	IV	2·006 ± 0·003	—	+0·075 ± 0·003	—	—
	V	2·006 ± 0·003	—	+0·010 ± 0·002	—	—

the time of writing both angular dependence and optical nuclear investigations are being carried out in order to solve these problems.

Mercier and Voitchovsky [68] have investigated the photoluminescence of the mixed crystals GaS_xSe_{1-x} for $0 < x < 1$ and have shown that the sharp lines from each crystal have similar excitation, polarization, temperature and time delay behaviour. Optical resonance studies of the mixed crystals currently being carried out at the University of Hull show that the results are very complicated but the triplet nature of the excitons can be followed through to GaS where preliminary details of the recombination processes have been reported by Dawson *et al.* [69]. GaS is an indirect band gap semiconductor with the layers arranged with β-polytype stacking. The high energy edge shows many absorption and emission lines and Aulich *et al.* [70], Razbirin *et al.* [71] and Belenkii and Godzhaev [72] have shown that these transitions

Fig. 23

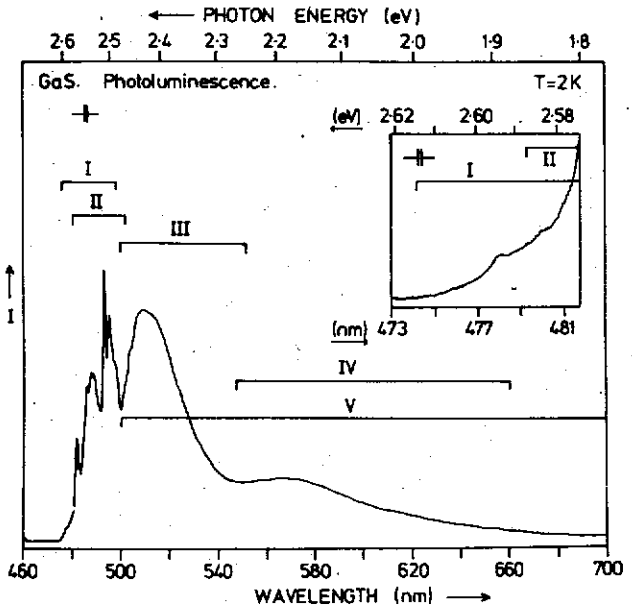

Luminescence of GaS at 2 K with inset showing the high-energy emissions in more detail. The emission regions labelled I to V correspond to the resonances illustrated in fig. 24.

are due to phonon assisted free and bound indirect exciton recombination. At longer wavelengths both sharp lines and broad bands are observed as shown in fig. 23 where the high-energy edge emission is shown in the inset.

For $B \| c$-axis five triplet exciton resonances were observed as shown in fig. 24 where the σ^- emission was monitored at the specified wavelengths. The resonances were labelled I to V and the emission regions associated with these resonances are shown in fig. 23. At the highest emission energies sharp (3·5 mT) exciton resonances

Fig. 24

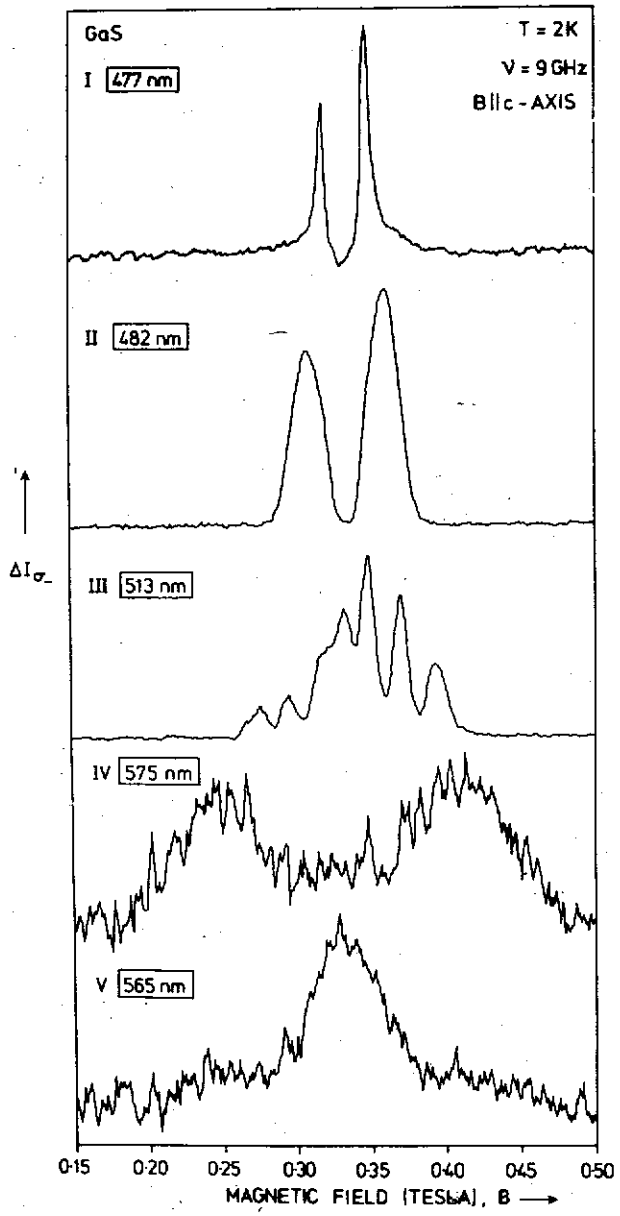

Triplet exciton resonances observed in GaS for $B \| c$-axis.

were observed and these were attributed to free indirect excitons. The remaining four resonances were attributed to bound indirect excitons. The resonances can be described by the hamiltonian, eqn. (4.1) where in each case $g_{ex\parallel}=2{\cdot}006\pm0{\cdot}003$ and the zero field splittings are $D^{I}=0{\cdot}013\pm0{\cdot}001\,cm^{-1}$, $D^{II}=0{\cdot}024\pm0{\cdot}001\,cm^{-1}$, $D^{III}=0{\cdot}025\pm0{\cdot}001\,cm^{-1}$, $D^{IV}=0{\cdot}075\pm0{\cdot}005\,cm^{-1}$ and $D^{V}=0{\cdot}010\pm0{\cdot}002\,cm^{-1}$. The type III resonance shows resolved hyperfine interaction and so a nuclear hyperfine term describing the interaction with one Ga nucleus must be added to the hamiltonian. So far angular dependence studies have been carried out in detail only on the type I spectrum. Figure 25 shows the typical axial behaviour of the spectrum giving $g_{\perp}=1{\cdot}87$. Comparing the resonances in fig. 17, 22 and 24 shows that the character of the GaS resonance is very different from those observed in GaSe. In the latter case the three levels show a small degree of thermalization so that a transition $|0\rangle\rightarrow|+1\rangle$ reduces the population of the $|0\rangle$ state and in turn the $|-1\rangle$ population also decreases as observed by the decrease of σ^{-} as shown in fig. 17. However, in GaS the resonances are observed to be almost the same strength for monitoring the σ^{+} and σ^{-} emission. This lack of dependence on the polarization can be explained in terms of mixing of the $|\pm1\rangle$ states by a strain field in the plane of the layers.

Fig. 25

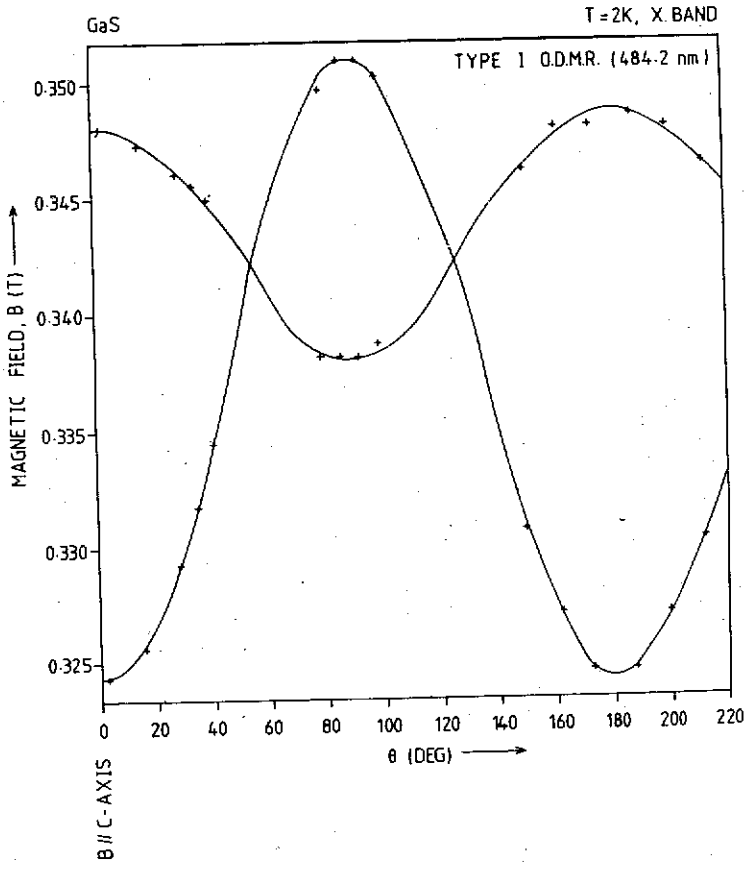

Angular dependence for B rotated away from the c-axis by angle θ for type I resonance in GaS.

The level crossing spectra shown in fig. 26 were obtained with a stress plate modulator and, because of overlapping emissions, more than one triplet system can sometimes be observed even when this overlap is not apparent from the resonance spectra. For example, the curve in fig. 26 (*e*) is a composite level crossing since if it compared with fig. 26 (*d*) the type IV level crossing is clearly observed with the type V crossing. Thus the single broad resonance (type V) is, in fact, made up of two triplet components with a zero field splitting of approximately 30 mT. Because both the σ^+ and σ^- emissions increase at resonance due to the thermal coupling between the ± 1 levels, the level crossing is more easily observed by monitoring either the σ^+ or σ^- emissions and not $(I_{\sigma+} - I_{\sigma-})$. (See Dawson *et al.* [66].)

Fig. 26

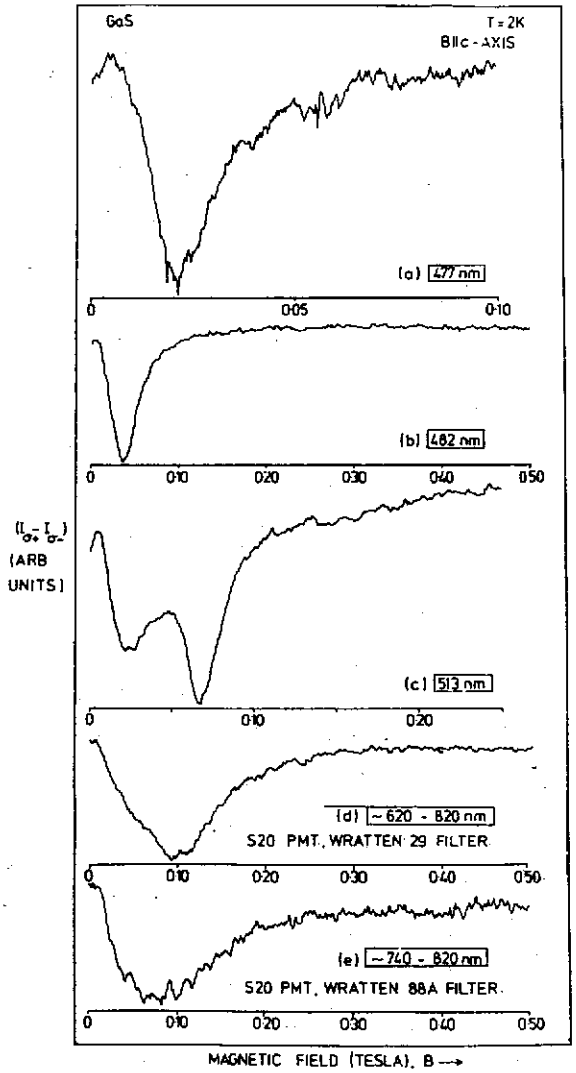

Level crossing measurements taken by monitoring $(I_{\sigma+} - I_{\sigma-})$ as a function of magnetic field for the emissions labelled in fig. 24. In general more than one level crossing is observed because of overlapping emissions.

The spectral dependence measurements were carried out at 0·5 nm intervals and the approximate regions for the resonances are shown in fig. 23. Since the five triplet excitons all have the same value of $g_{ex\parallel}$ it is assumed that the same indirect excitons are recombining under different environmental conditions. In fact, type II and type III resonances have the same D value suggesting that the difference lies in the strengths of the hyperfine interactions—resolved in the type III but not in the type II. Since this interaction involves only one Ga nucleus ($I=\frac{3}{2}$) the type III resonance is consistent with an exciton bound at a Ga-vacancy. The angular dependence of the spectrum, in so far as it can be followed for this spectrum, shows that the centre is axial along the c-axis in agreement with this model. (See Killoran *et al.* [73] and table 1 for a summary of the parameters.) Some crystals showed only the type I resonance and spectral dependence measurements showed that this resonance came not only from the high-energy wing but was also observed on the M_1 line and phonon replicas. These resonances have been attributed to free indirect excitons because of the narrowness of the lines (3·5 mT). If the exciton is localized the width of the resonance is expected to be large since lattice distortions at the different sites would produce different values of the zero field splitting. Also, since the Ga nuclei have a nuclear spin, the width of the resonances can also be large because of unresolved hyperfine interactions. However, a free exciton moving through the lattice is subject only to the average crystal field and hyperfine interactions; in both cases the fluctuations average to zero and the resonances are motionally narrowed. The zero field splitting of the triplet state then corresponds to that due to the undistorted lattice and D^{I} is a fundamental parameter of the crystal. The free exciton resonances will be observed on the bound exciton emissions when the spin polarization of the free exciton is partly retained on capture.

§5. Donor–acceptor recombination

5.1. *Introduction*

Electron–hole recombination can take place between donor–acceptor pairs with different separations and so the luminescence is made up of many contributions with energies dependent on the separation as

$$E=E_{\mathrm{g}}-E_{\mathrm{d}}-E_{\mathrm{a}}+\frac{e^2}{\varepsilon r} \tag{5.1}$$

and radiative transition probabilities also dependent on the separation

$$W(r)=W_0\exp\left(-\frac{2r}{a_0}\right), \tag{5.2}$$

where a_0 is the Bohr radius and W_0 is a constant, the transition probability as $r\to 0$. The positive sign of the Coulomb term in eqn. (5.1) reflects the fact that in the final state the donor–acceptor pairs are ionized, i.e.

$$(\mathrm{D}^0,\mathrm{A}^0)\to(\mathrm{D}^+,\mathrm{A}^-)+h\nu.$$

Donor–acceptor recombination was first investigated in GaP where the emission consists of many sharp lines, each corresponding to one value of the separation [74]. The emissions are only discrete for near pairs while for distant pairs the recombination is in the form of a broad band with LO phonon replicas at lower energies. These emissions are seen clearly in the II–VI crystals such as the green edge emission in CdS

and the blue edge emission in ZnSe. Details of the investigations of the donor–acceptor emissions in both III–V and II–VI compound crystals can be found in the comprehensive review by Dean [75]. At longer wavelengths, particularly in the II–VI compounds there are many broad emission bands which have also been attributed to donor–acceptor pairs. Since the recombination time increases with increasing separation a time-resolved luminescence measurement will show the emission peak to move to lower energy as the delay is increased. Also, the emission peak moves to higher energy as the excitation power is increased because distant pairs (with lower energy) saturate first. Therefore, even without the sharp line donor–acceptor pair series which can be related to the distant pair broad bands it is possible to determine the donor–acceptor nature of a broad emission. These mid-band gap emissions may be due to deep donor–acceptor or donor–deep acceptor transitions. Cavenett and Hagston [76] investigated the broad edge emission in ZnSe and showed that the donor and acceptor g-values could be obtained from a magneto-circular-polarization measurement. This work was followed by optical magnetic resonance studies on a wide range of emission bands in II–VI crystals. We will see, in particular, that the character of the donor–acceptor recombination giving rise to the edge emission is quite different from the donor–acceptor recombination involving deep states. In the former case the donor–acceptor pairs are thermalized and the resonances of the shallow acceptors, which have the symmetry of the upper valence band, are generally not observed. These measurements provide a very straightforward method of measuring the donor or electron g-value. In the case of the deep state the investigations are important because the deep acceptor resonances can be observed and, knowing the shallow donor depth, the position of the deep acceptor in the band gap can be obtained. These donor–acceptor recombinations usually involve unthermalized pairs and, as discussed previously, very large O.D.M.R. signals can be obtained.

Since the recombination time of a donor–acceptor pair depends on the donor–acceptor separation it is also possible to explore the interaction between near pairs by using the pulsed O.D.M.R. technique to carry out time resolved O.D.M.R. [77]. The pulsed system can also be used to estimate the spin lattice relaxation time when $T_1 < \tau$ [78].

5.2. *Donor resonance from shallow donor–acceptor pairs*

5.2.1. *CdS*

The green edge emission in CdS is shown in fig. 27 (a) and consists of two sets of emission bands. The high-energy emission and LO phonon replicas are due to free electron to acceptor recombinations (no shift of the emission peak is found in time resolved emission measurements). The low energy series is the distant donor–acceptor emission.

CdS crystals have hexagonal structure with C_{3v} symmetry. The conduction band is slightly anisotropic with a minimum at $k=0$ and $S=\frac{1}{2}$. The upper valence which is degenerate at $k=0$ for tetrahedral symmetry is split in the lower symmetry so that there are three bands, Γ_9, Γ_7, Γ_7. The acceptor level is derived from the upper valence band with wave functions $\phi_{\pm 3/2}$ ($J=\frac{3}{2}$). For an external magnetic field set parallel to the c-axis the allowed donor–acceptor recombinations are as shown in fig. 1 (a) which is reproduced from the first O.D.M.R. study of CdS by Brunwin *et al.* [79]. The emission is circularly polarized. Figure 28 shows the same recombination process using another notation after Dunstan *et al.* [80]. Here the neutral donor and

Fig. 27

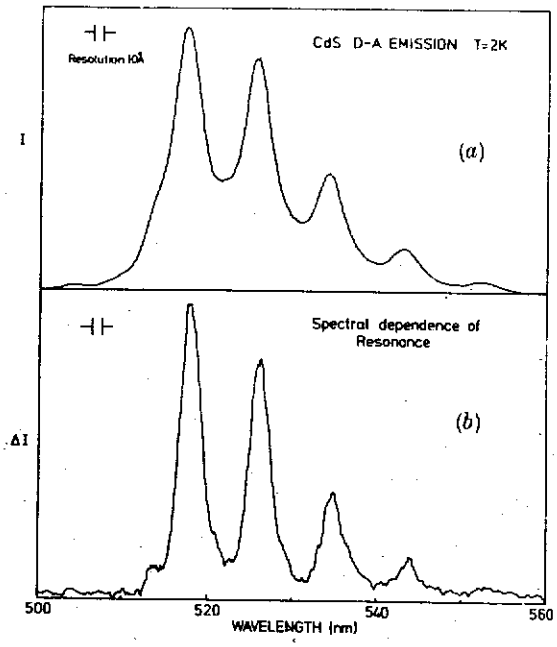

(*a*) Green edge emission in CdS due to shallow donor to shallow acceptor transitions and free electron to acceptor transitions at higher energy. (*b*) Spectral dependence of the donor resonance illustrated in fig. 29.

Fig. 28

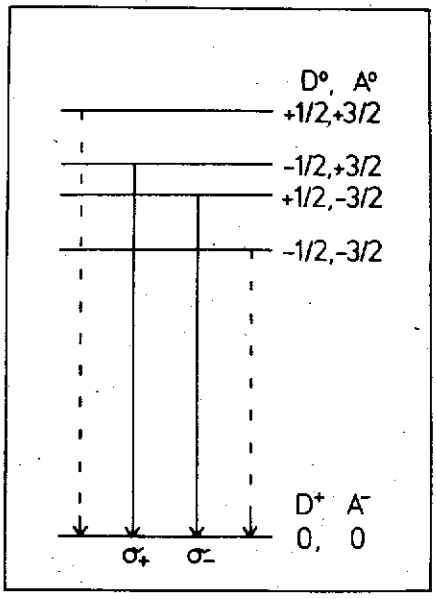

Energy level scheme for a weakly exchange coupled donor–acceptor pair in CdS. The hole is labelled by the unpaired electron spin and the ground state is diamagnetic. (Compare with fig. 1 (*a*).)

acceptor are considered as a weakly coupled pair which is the excited state of the system. The ground state is the ionized pair (D^+, A^-). The hole is labelled by the unpaired acceptor electron and the optical transitions are the same as in fig. 1 (*a*). If the green emission is monitored in a direction parallel to both B and the c-axis then the donor optical resonance is observed as changes in the intensities of the circularly polarized components as shown in fig. 29. $I_{\sigma-}$ increases by 0·05% and $I_{\sigma+}$ decreases by a similar magnitude. A spectral dependence measurement of the donor resonance shows that only the donor–acceptor pair bands give the resonance and so only the thermalized donor electrons are observed at resonance as shown in fig. 27 (*b*). Attempts have been made to observe the free electron resonance on the free-to-bound transitions by optical pumping techniques, since circular polarization measurements confirmed that there was high-spin memory on the free-to-bound emissions. However, no resonance has been seen. The measured g-values were $g_{\parallel}=1{\cdot}789\pm0{\cdot}002$ and $g_{\perp}=1{\cdot}769\pm0{\cdot}002$ in agreement with previously published values [81–83]. If the microwaves saturate the donor resonance transitions $n_3=n_4=n$ and $\Delta I_{\sigma-}/I_{\sigma-}=-\Delta I_{\sigma+}/I_{\sigma+}=10\%$ for a thermalized doublet. Since the circular polarization measurements indicated that the donors were not totally thermalized and because the observed resonance could not be saturated with the available microwave power, the observation of the much smaller values of $\Delta I/I$ can be understood.

In the original investigations no acceptor resonances were observed and this was attributed to the forbiddenness of the $\Delta M_J=\pm3$ transitions between the $\phi_{\pm3/2}$ states. However, recent measurements by Patel *et al.* [84] have shown that the resonance can be observed, particularly with B away from the c-axis. This work follows the results obtained on SiC by Dang *et al.* [85] who were the first to observe shallow acceptors by O.D.M.R. It is valuable to note the importance of the axial field

Fig. 29

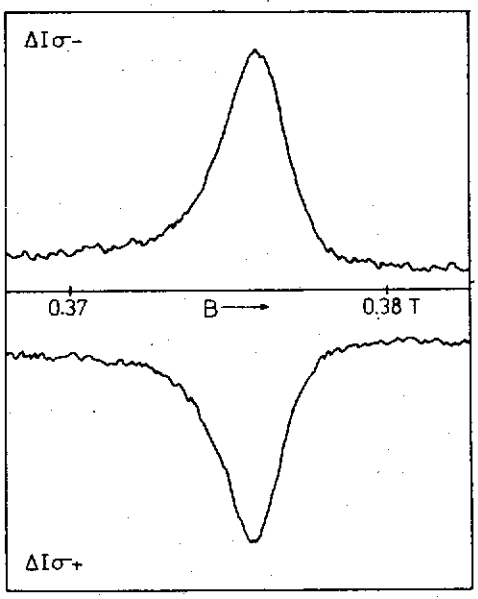

O.D.M.R. signals of the donor in CdS showing the polarization dependence of the signal characteristic of a thermalized donor.

in these crystals since the removal of the acceptor state degeneracy reduces the broadening effect of random strain on the resonances.

5.2.2. *ZnSe*

The edge emission in ZnSe has been investigated in considerable detail since the sharp donor–acceptor pair spectra were reported by Dean and Merz [86] and Merz *et al.* [87]. In analogy with CdS the close donor–acceptor pairs give rise to many sharp emissions and the distant pairs produce a broad band at 2·70 eV with LO phonon side bands at lower energy. O.D.M.R. of the donor resonance was reported by Dunstan *et al.* [88] who monitored the donor–acceptor emission in a direction parallel to the magnetic field. As in the case of CdS the signal at $g_e = 1{\cdot}15 \pm 0{\cdot}010$ was polarization dependent with $I_{\sigma+}$ decreasing and $I_{\sigma-}$ increasing by 0·1%. The spectral dependence was measured for the electron resonance and reported for high U.V. excitation intensities in Dunstan *et al.* [52]. Only the donor–acceptor transitions showed the electron resonance. The recombination model for electron–hole recombination is shown in fig. 31 where the excited state describes a weakly coupled donor–acceptor pair with $S = \frac{1}{2}$ for the electron and $J = \frac{3}{2}$ for the hole [76, 52]. Assuming a thermalized pair model calculated values of $\Delta I_{\sigma+}/I_{\sigma+} = -5{\cdot}0\%$ and $\Delta I_{\sigma-}/I_{\sigma-} = 6{\cdot}3\%$ are found for microwave saturation of the donor resonance. No shallow acceptor resonances were observed [76] but random strains in the cubic crystals would perturb the acceptor levels making the resonance too broad to detect.

5.2.3. *ZnTe*

The edge emission in ZnTe has been investigated by magneto-optical measurements in order to determine the conduction on valence band g-values. These measurements are summarized in the paper by Killoran *et al.* [89] who investigated O.D.M.R. in ZnTe crystals prepared at Grenoble from Te rich ZnTe melts. The emission is shown in fig. 31 and labelled according to Dean *et al.* [90] who investigated

Fig. 30

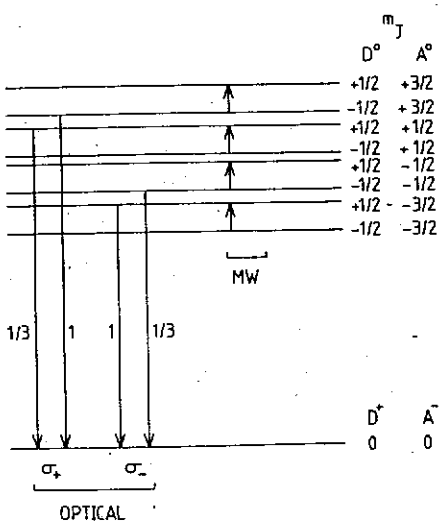

Energy level schemes for a donor–acceptor pair in a semiconductor with T_d symmetry such as ZnSe, ZnTe and CdTe. The hole is described by $J = \frac{3}{2}$ from the upper valence band.

Fig. 31

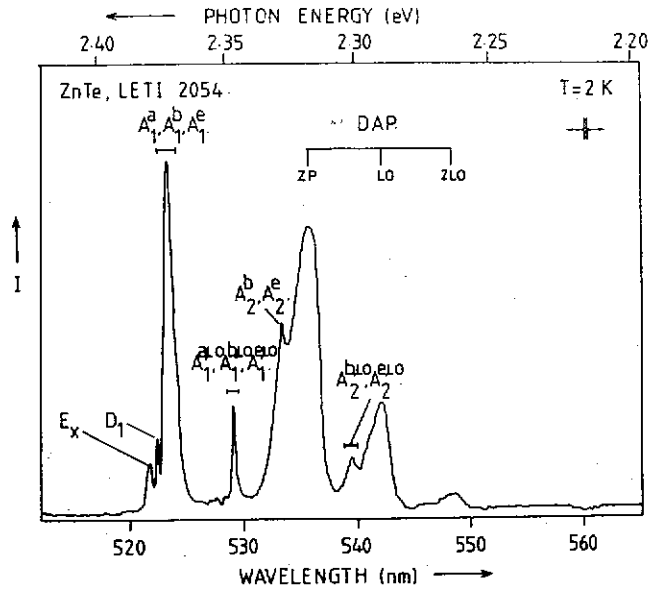

Luminescence from ZnTe single crystals showing bound exciton and donor–acceptor pair luminescence. (Labelling after Dean *et al.* [90].)

the optical properties of this material in detail. In particular, the donor–acceptor recombination has been attributed to $|Li|_{Zn}$ and $|P|_{Te}$ with the donors unidentified.

Using a high resolution spectrometer it was shown by Killoran *et al.* [89] that the O.D.M.R. signal, shown in fig. 32, came from the 2·250–2·325 eV region. The method of measurement was similar to that already described for CdS and ZnSe above but in the case of ZnTe the best signal-to-noise was obtained by using sub-band gap excitation (520 nm from a krypton laser) when the non-resonant background signal was small. Figure 32 shows that the resonance was observed as a change in the polarization of the emission and $g_e = +0{\cdot}401 \pm 0{\cdot}004$. The magnitude of the changes was measured to be $\pm 0{\cdot}05\%$ whereas, using the model already discussed for ZnSe in fig. 30 changes of $\Delta I_{\sigma+}/I_{\sigma+} = -3{\cdot}8\%$ and $\Delta I_{\sigma-}/I_{\sigma-} = +7{\cdot}0\%$ assuming $g_h = +0{\cdot}6$ [91].

The observed value of g_e from the O.D.M.R. measurements confirms the recent magneto-optical measurements by Tews [92] who could explain the Zeeman data for selectively excited donor–acceptor pair lines only by assuming a positive value for g_e in contrast with the previous measurements which suggested that the sign was negative [90].

5.3. *Donor–deep acceptor recombination processes*

5.3.1. *ZnS* : $(V_{Zn}-Cl)$

Investigations of the broad bands in ZnS by James *et al.* [93–94] were the first to show that O.D.M.R. could be used to investigate donor–deep acceptor transitions. In particular, a study of the anisotropy of the acceptor O.D.M.R. spectra allowed the identification of the centre and by assuming the depth of the donor and estimating the zero-phonon energy of the donor–acceptor transitions the depth of the acceptor was found.

Fig. 32

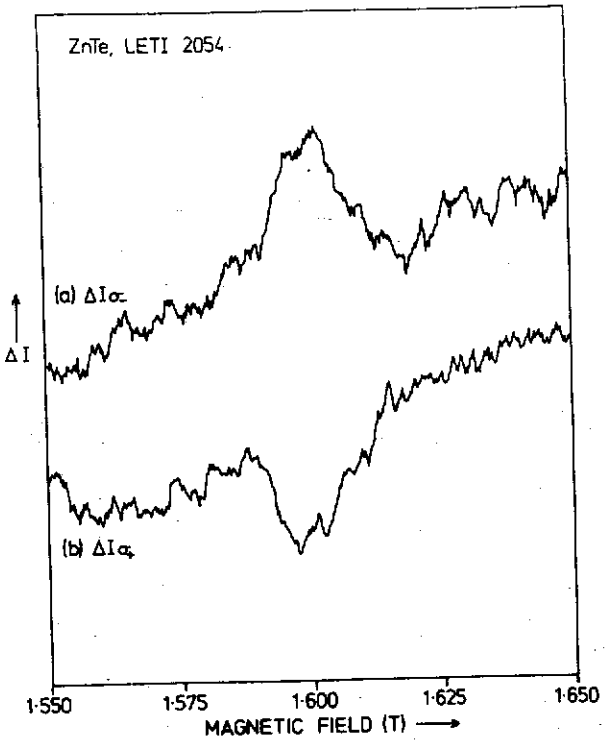

Optical resonance signals in ZnTe obtained by monitoring the donor–acceptor pair emission shown in fig. 31. The polarization properties are consistent with the model shown in fig. 30.

The origin of the self-activated blue emission in ZnS had been a matter of considerable controversy. On the one hand some authors, for example, Shinoya *et al.* [95] favoured a model in which transitions occurred within the level scheme of an isolated centre such as the $(V_{Zn}–Cl)'$ pair. In contrast the donor–acceptor model was favoured by Era *et al.* [96] who investigated the time resolved emission spectra and showed that the results were consistent with donor–acceptor pair recombination. Watkins [97] showed that the alignment properties of magnetic centres called A-centres and the polarization of the self-activated emission depended in a similar fashion upon the wavelength of the exciting light and suggested an association between these centres and the self-activated emission. Kasai and Otomo [98] were the first to observe E.S.R. from ZnS showing self-activated emission and the axially symmetric centre was called the A-centre. Detailed studies by Rauber and Schneider [99], Schneider *et al.* [100], Dischler *et al.* [101], and Holton *et al.* [102] showed that two types of A-centre can be identified as illustrated in fig. 33 (*a*) and (*b*). In fig. 33 (*a*) the centre (V_{Zn}–Cl) is shown while in fig. 33 (*b*) a centre involving Al donors, (V_{Zn}–Al), is shown. Details of the E.S.R. data can be found in the reviews by Schneider [19] and Watts [103].

O.D.M.R. investigations reported by James *et al.* [93–94] and Nicholls *et al.* [104] showed that both donor and A-centre acceptors were involved in the self-activated emission confirming the donor–acceptor nature of the transitions. The O.D.M.R.

Fig. 33

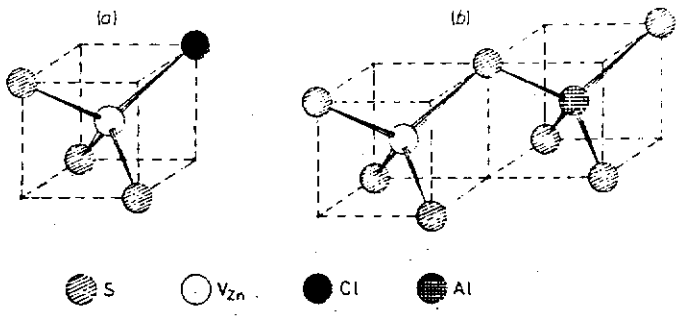

The chlorine (*a*) and the aluminium (*b*) A-centres in ZnS.

spectra for hexagonal ZnS is shown in fig. 34. The high field resonance was found to be isotropic with $g = 1{\cdot}886 \pm 0{\cdot}003$ and corresponds to a donor resonance. The low field resonances were found to be anisotropic and a comparison of the experimental angular dependence of the resonance with line shapes calculated using g-values of $g_{\parallel} = 2{\cdot}006 \pm 0{\cdot}003$ and $g_{\perp} = 2{\cdot}052 \pm 0{\cdot}003$ showed the centre to be axially symmetric with $g_{\parallel}$ along one of the four bond directions. These results were compared with that of Schneider *et al.* [100] and it was concluded that the acceptor was the chlorine A-centre. Spectral dependence measurements showed that both the donor and acceptor resonances came from an emission at 2·70 eV. The excitation and emission processes are shown in fig. 35. U.V. light removes an electron from the (V_{Zn}–Cl) self-activated centre (which is diamagnetic) leaving the paramagnetic A-centre and an electron on a donor. The self-activated emission occurs when the electron and hole recombine as shown in the second diagram. Similar investigations were carried out in cubic ZnS with aluminium added as a donor. Details of these investigations can be found in Nicholls *et al.* [104] and the magnetic resonance data is summarized in table 2.

Fig. 34

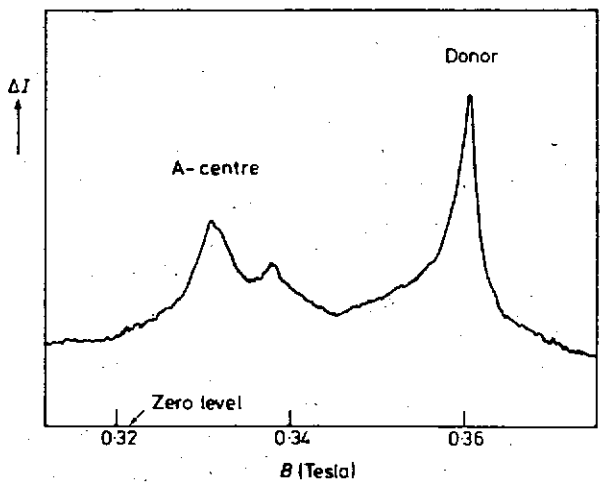

O.D.M.R. observed in hexagonal ZnS for $B \| c$-axis when monitoring the total emission.

Fig. 35

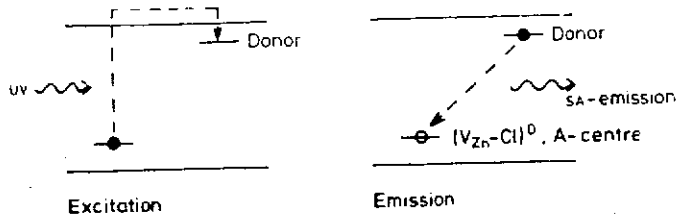

Excitation and emission model for the donor–deep acceptor emission in ZnS. An electron is excited to the conduction band from the diamagnetic self-activated centre leaving the paramagnetic A-centre acceptor.

Table 2. Magnetic resonance parameters for vacancy and vacancy-associated centres in II–VI single crystals.

Material	Model	Label	g_1 ($g_\parallel$)	g_2 ($g_\perp$)	g_3	Temp. (K)	Exp.	Reference
ZnS (cubic)			2·0031	2·0501	2·0568	1·3	E.S.R.	[100]
ZnS (cubic)			2·0530	2·0286		77·0	E.S.R.	[99]
ZnS (hex)	(V_{Zn}–Cl)	A1	2·0592	2·0287		77·0	E.S.R.	[100]
ZnS (hex)	(V_{Zn}–Cl)	A2	2·0192	2·0404	2·0603	77·0	E.S.R.	[100]
ZnS (hex)	(V_{Zn}–Cl)	A	2·0060	2·0520		1·8	O.D.M.R.	[104]
ZnSe	V^-	V	1·9548	2·2085			E.S.R.	[123]
							O.D.M.R.	[125, 126]
	$(V–Te)^-$	X	1·8731	2·2575			E.S.R.	[123]
	$(V–S)^-$	A2	1·9604	2·1450	2·2590		E.S.R.	[123]
	$(V–Cl)^0$	A1	1·9503	2·1549	2·2488		E.S.R.	[123]
			1·9597	2·1612	2·2449		E.S.R.	[122]
							O.D.M.R.	[121, 52]
							O.D.M.R.	[125, 126]
	(V–X)	A3	1·9616	2·2045	2·2162		E.S.R.	[123]
	(V–X)	A4	1·9579	2·1655	2·2348		E.S.R.	[123]
	(V–X)	Y	2·2703	2·1612	2·2923		E.S.R.	[123]
ZnTe	(V_{Zn}–Al)	A	2·0450	2·0880	2·0910		E.S.R.	[191]

In contrast to the polarization dependent O.D.M.R. signals discussed at the beginning of this section for donor–shallow acceptor transitions the O.D.M.R. signals in ZnS were total intensity increases in the luminescence at resonance. At first it was thought that thermalized donor–acceptor pair transitions were involved [93, 94] but it became clear from other investigations, particularly from pulsed O.D.M.R. experiments (see Dawson and Cavenett [77]) that a thermalized donor–acceptor pair model could not explain the magnitude of the O.D.M.R. signals and it is now recognized that the unthermalized model discussed in fig. 1 (*b*) is appropriate. A rate equation analysis for both the thermalized and unthermalized cases for a donor–acceptor pair has been given in Nicholls *et al.* [104] whereas a more detailed description including analysis of the O.D.M.R. signal waveform has been given by Dunstan and Davies [105]. The analysis of the donor–acceptor pair recombination is based on the energy level scheme shown in fig. 36. The four levels represent the states in a magnetic field for two weakly coupled spin $\frac{1}{2}$ centres; the energies are given on the diagram. The hole is labelled by the unpaired spin at the acceptor and the allowed

Fig. 36

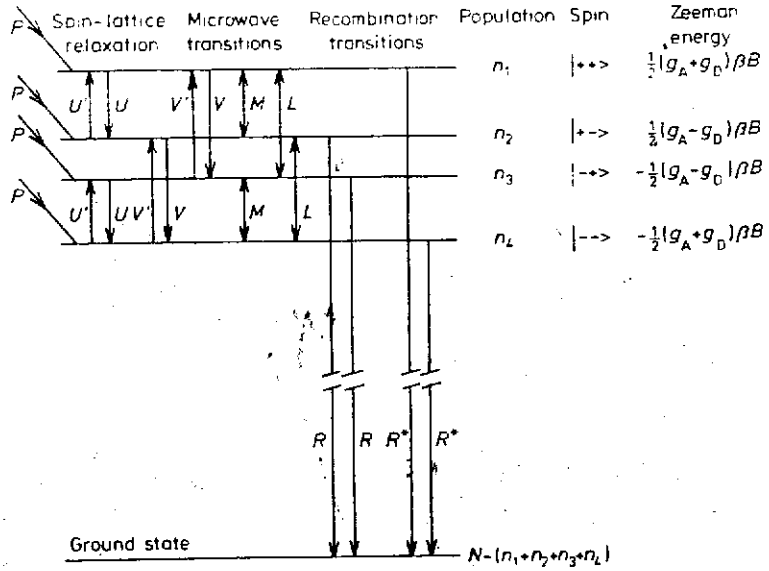

Energy level scheme for a donor–acceptor pair in a magnetic field showing transitions within the donors as U, U' and M and within the acceptors as V, V' and L.

transitions conserving spin are from the two central levels ($M_S=0$) and the transitions are labelled R. It is expected that these transitions are principally radiative. Conversely, the transition rates for the outer states are R^* and its is assumed that these are mainly non-radiative. Spin lattice relaxation occurs with rate constants U, U' for the donors and V, V' for the acceptors while the rates for the donor and acceptor resonances are M and L respectively. If $R \gg R^*$ the inner two levels are less populated than the outer two levels and microwave transitions tend to equalize the populations and increase the emission intensity. For R^* entirely non-radiative and $R \gg R^*$ the signal is

$$\frac{\Delta I}{I} = \frac{R-R^*}{R+R^*} \quad \text{at low optical excitation}$$

and

$$\frac{\Delta I}{I} = \frac{R-R^*}{2R^*} \quad \text{at high optical excitation.}$$

Clearly in the latter case for R^* small, the signals can be very large. However, it should be noted that since in a given sample there are donor–acceptor pairs of different separations and so the recombination rates R and R^* will have a wide range of values. Thus the observed signal may contain contributions from both thermalized and unthermalized pairs.

5.3.2. *ZnS : Ga and ZnS : In*

The emission bands excited in ZnS crystals doped with Ga have been reported by several authors [106, 107] showing that emission bands around 2 eV are associated with this particular donor. Rauber and Schneider [108, 109] and Holton and Watts

[110] have shown that the electron on the Ga^{2+} ($^2S_{1/2}$) donor is well localized implying that it is a deep donor in contrast with chlorine and aluminium. Davies and Nicholls [111] investigated the recombination processes in this material by O.D.M.R. and observed a donor–acceptor process involving Ga donors and A-centre acceptors. The O.D.M.R. spectrum observed with an S20 photomultiplier from these crystals is shown in fig. 37. The anisotropic resonance at 0·33 T was shown to be the A-centre (V_{Zn}-donor), acceptor discussed above while the other resonances, which were found to be isotropic, corresponded to the Ga^{2+} resonances, which were found to be isotropic, corresponded to the Ga^{2+} resonances previously reported [108–110]. As indicated in the diagram the doublet structure of the low field transitions is due to the mixed cubic and hexagonal quality of the crystals. The energy level scheme for the ^{71}Ga nuclear spin of $I=\frac{3}{2}$ is shown in fig. 34 where $F=I+S$, the total angular momentum, and M_F, the corresponding magnetic quantum number, are appropriate for the low magnetic field limit. For the Ga-donor $F=2$ or 1 and the observed microwave transitions observed by Davies and Nicholls [111] at X and K band are shown in fig. 38. Spectral dependence measurements confirmed that the A-centre and Ga resonance came from the same band at 1·94 eV, thus establishing the donor–acceptor nature of the transition. Using the known depth of the A-centre of 0·95 eV, the depth of the donor was estimated to be 0·4 eV below the conduction band in agreement with the value of 0·42 eV given by Apple and Williams [112]. The optical resonance signals which were increases in the emission intensity were interpreted in terms of an unthermalized donor-acceptor pari model as discussed for ZnS. However, when hyperfine interaction is present the energy level scheme is more complicated and in this case the levels are labelled by $|F, M_F, M_A\rangle$. By a consideration of the relative emission rates from the different levels, the observed O.D.M.R. signals can be explained and the microwave emission E.S.R. signal for the low field Ga resonance observed by Holton and Watts [110] can be understood.

Fig. 37

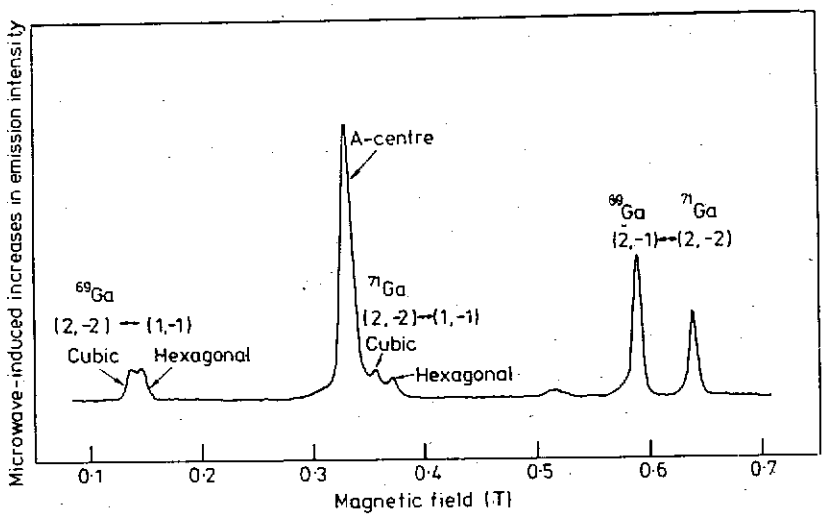

O.D.M.R. signals for ZnS : Ga at 2 K. The microwave induced transitions for the two Ga isotopes are shown and the resonances marked cubic and hexagonal refer to signals in the different phases of the material. (After Davies and Nicholls [111].)

Fig. 38

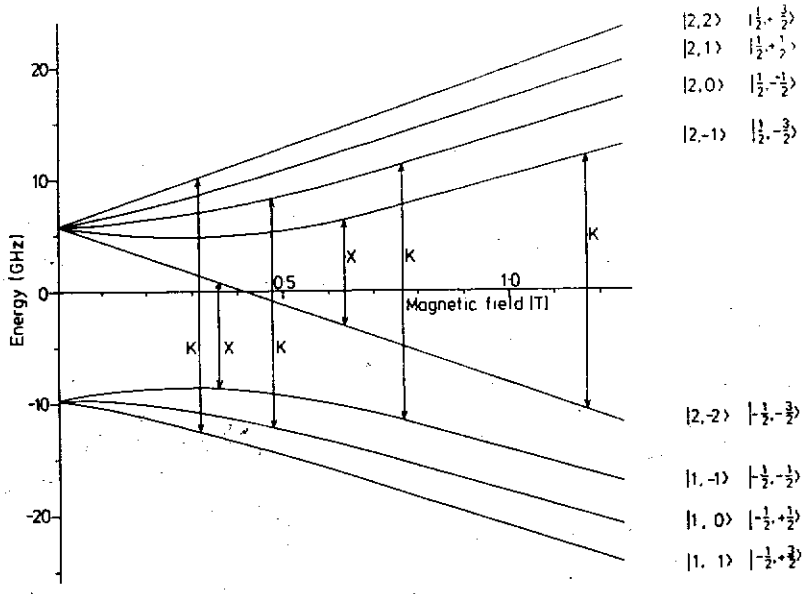

Energy levels for the $^{71}Ga^{2+}$ donor in cubic symmetry; $A = 7{\cdot}716$ GHz, $g = 1{\cdot}9974$. The states are marked in both the very-low-field notation $|F, m_F\rangle$ and in the high-field notation $|M_0 m_I\rangle$. The transitions observed at X and K bands are shown. (After Davies and Nicholls [111].)

The behaviour of In as a deep donor in ZnS is similar to Ga. An emission band at 1·94 eV has been shown by Nicholls and Davies [113] to be due to transitions involving In donors and A-centre acceptors, suggesting that the In and Ga donors are both at 0·4 eV from the conduction band. In the case of In, a single resonance was observed by Rauber and Schneider [108] in conventional E.S.R. but three transitions were observed in the O.D.M.R. spectrum by Nicholls and Davies [113] who suggested that the In on the Zn sites was associated with a defect or vacancy at a nearest cation site. A second emission band at 2·34 eV was also shown to involve the In donors but the acceptor was unidentified.

5.3.3. *ZnO : Li*

Lithium doped ZnO shows a yellow luminescence which has been investigated by several authors [114–116]. The Li^+ ion substitutes for Zn^{2+} forming the ionized acceptor Li^- or, under photo-excitation, the neutral Li^0 which is paramagnetic and has been investigated by Shirmer [117]. Cox *et al.* [118] and Block *et al.* [119] investigated the yellow luminescence by O.D.M.R. and observed a donor resonance at $g = 1{\cdot}957 \pm 0{\cdot}001$ and for $B \| c$-axis two Li acceptor resonances corresponding, for one line to the hole localized on the oxygen that lies along the c-axis and, for the other line to the hole localized on one of the three remaining oxygen atoms, in agreement with the E.P.R. results [117]. The investigation confirmed that the luminescence centres at 575 nm is donor–acceptor in nature. The O.D.M.R. results were interpreted in terms of an unthermalized donor–acceptor model as discussed in the previous section. An important aspect of this study was the observation of strong

broadening of the O.D.M.R. signals under high microwave power. The broadening was explained in an exchange interaction which depends on the donor–acceptor separation.

5.3.4. *ZnSe : (V_{Zn}–Cl) and V_{Zn}*

The investigation of the vacancy associated defects in ZnSe was a natural extension of the studies of ZnS and O.D.M.R. measurements were carried out on the broad emissions in the 620–630 nm region by Dunstan *et al.* [52, 120] and Nicholls *et al.* [121]. The crystals were grown either by iodine vapour transport or from the melt in a high-pressure furnace. The latter has the advantage that dopants, particularly metals such as copper, can be easily incorporated into the material. In ZnSe : Cu,I material two emission bands at 570 nm and 650 nm were observed. The O.D.M.R. signals observed included a broad isotropic donor resonance at $g_e = 1{\cdot}135 \pm 0{\cdot}010$ and a group of anisotropic lines near $g = 2$. Angular dependence studies of these acceptor resonances are shown in fig. 39 where the observed resonance (centre traces) is compared with the calculated lines shapes for the A-centre g-values (upper traces) which had been reported by Holton *et al.* [122] and Watkins [123] and the V^--centre g-values from the work of Watkins [124]. The comparison rules out the A-centre and Dunstan *et al.* [120] attributed the resonance to the isolated zinc vacancy with $g_\parallel = 1{\cdot}9548$ and $g_\perp = 2{\cdot}2085$. The spectral dependence measurements of the

Fig. 39

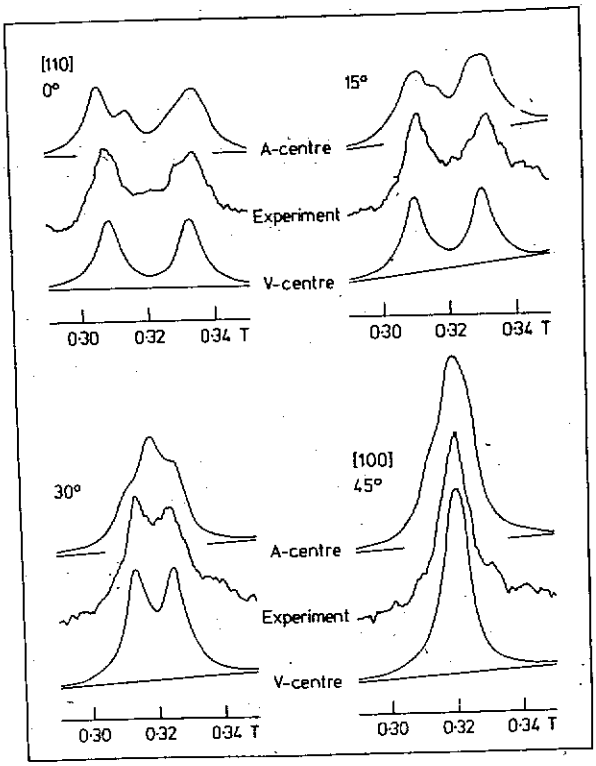

Angular dependence of the O.D.M.R. acceptor signal in ZnSe : Cu,I. The central trace is the experimental result, the upper trace is the line shape calculated from the A-centre (A1, table 1) and the lower trace from the V^- centre.

acceptor resonances showed that a band centred at 632 nm. This observation caused considerable controversy since it was not expected that the V^--centre would be stable in as grown material and, in fact, Watkins [124] had observed the resonances from these centres only in irradiated samples. The controversy was resolved by Lee *et al.* [125, 126] who investigated by O.D.M.R. the irradiated crystals from Watkin's original experiments [124]. The results are shown in fig. 40 for a microwave frequency of 35 GHz. Trace (*a*) shows both the donor and acceptor resonances, the former being very strong since all emissions were donor–acceptor in nature. In trace (*b*) all the acceptor resonances (A-centre and V^-) are shown while in trace (*c*) the band at 720 nm was monitored and only the V^--centre resonances are observed. The high quality of the crystal and the resolution obtained at 35 GHz establishes the identity with certainty. Dunstan *et al.* [52] have assigned their O.D.M.R. spectrum to a vacancy–defect pair such as the A3 centre reported by Watkins [123] which is thought to be associated with aluminium [126]. A summary of the various centres observed in ZnSe by magnetic resonance can be found in table 2.

The A-centre (or A1 centre, table 2) has been observed by O.D.M.R. and reported by Nicholls *et al.* [121], Dunstan *et al.* [52] and Lee *et al.* [125, 126]. This is the vacancy–chlorine pair centre analogous to that shown in fig. 33 (*a*). The magnetic resonance information shows the centre to be orthorhombic with $g_1 = 1{\cdot}9597$, $g_2 = 2{\cdot}1612$ and $g_3 = 2{\cdot}2449$ and twelve lines are possible in the resonance spectrum corresponding to there being 4 nn sites for the Cl ion by the vacancy and the hole being localized on one of the three selenium neighbours. For the magnetic field near the principal axis of [111] the resonance spectrum consists of three lines as shown in

Fig. 40

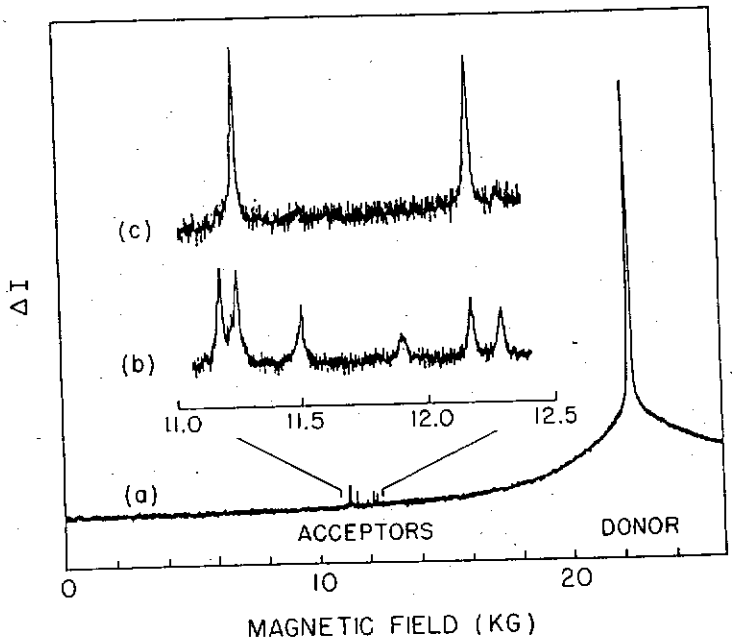

O.D.M.R. signals at 35 GHz from irradiated ZnSe showing in (*a*) both the donor and acceptor resonances, in (*b*) the V^- and A-centre resonances and in (*c*) the V^- centre signals. (After Lee *et al.* [125].)

fig. 41 from Dunstan *et al.* [52]. The lower trace is the calculated spectrum for the A1-centre using the above g-values. Spectral dependence measurements by both groups show that the A1-centre is the acceptor of a donor–acceptor recombination process at 620 nm.

5.3.5. *ZnSe: P*

Phosphorus doped ZnSe crystals have been investigated by Reinberg *et al.* [127] who showed that an emission at 1·91 eV correlated with the magnetic resonance measurements of Watts *et al.* [128] who deduced that a photo-enhanced E.S.R. spectrum was due to P_{Se}-centres with C_{3v} Jahn–Teller distorted symmetry. Davies and Nicholls [129] and Nicholls and Davies [130] investigated by O.D.M.R. ZnSe : Ga, P crystal material which showed the same emission and E.S.R. spectra as described above. Both electron and phosphorus acceptor resonances were observed as increases in the luminescence and these results were interpreted in terms of the unthermalized donor–acceptor pair model discussed above for ZnS. The authors concluded that the 1·91 eV emission resulted from donor–acceptor recombination with the P_{Se}-centres acting as deep (~0·6–0·7 eV) acceptors.

5.4. *Summary*

The studies of donor–acceptor recombination by O.D.M.R. will always have an important place in the general field of O.D.M.R. in semiconductors since many of the basic techniques were developed through these investigations. In general the acceptor resonance can be identified from angular dependence studies and the spectral dependence of the acceptor resonance allows the donor–acceptor process to be associated with a particular emission band, even when this band is overlapped by other emissions. Therefore, if an assumption is made concerning the energy of the

Fig. 41

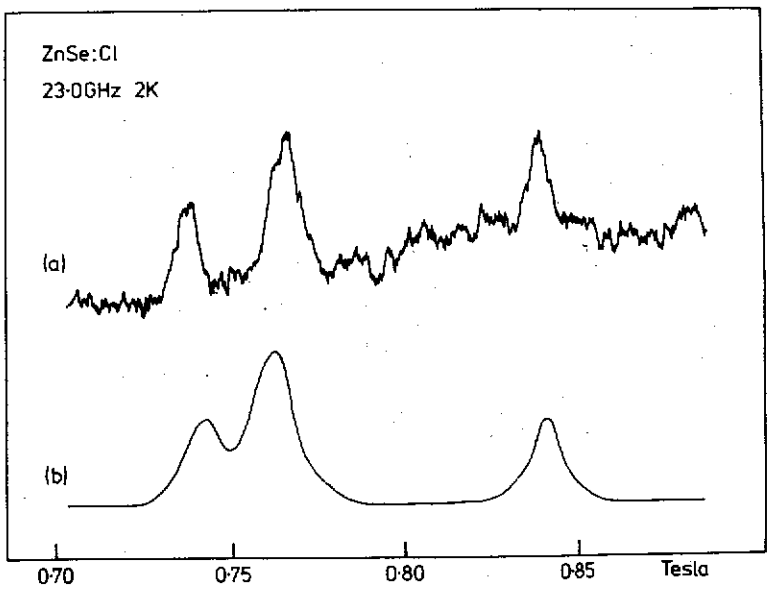

O.D.M.R. signals from ZnSe:Cl at 9·5 GHz for $B \| [111]$ showing the experimental and calculated resonances of the A-centre (A1).

zero-phonon transition for a broad band, the depth of either the donor or acceptor level in the band gap can be estimated if the energy of one of the levels is known. This is important for comparison with photocapacitance studies which also determine the depths of defects in semiconductors. Some caution should be exercised on making this comparison since the spectral dependence senses those centres which respond well under the experimental conditions, particularly the chopping frequency. However, time resolved emission and O.D.M.R. measurements show a wide range of lifetimes which are related to the different donor–acceptor separations. Therefore, the spectral dependence may not include all of the emission band involved with a particular donor–acceptor recombination.

A second caution relates to the definite assignment of a donor–acceptor emission band peak to a particular acceptor centre. This point is made clear by the study of the ZnSe centres which show that overlapping emissions can be attributed to different forms of the same centre, i.e. donor–acceptor transitions associated with several (vacancy–donor) acceptors. Thus the observation of different emission bands by various authors for the same dopant probably indicates the different preparation method of the crystals and different impurity content. For example, the emission bands reported for ZnS : Ga, namely 2·02 eV [106], 1·86 eV [107], 1·94 eV [111] clearly all involve a Ga-donor to acceptor transition where the precise nature of the acceptor, for example an A-centre, depends on the crystal structure and impurity content. O.D.M.R. studies of donor–acceptor recombination have mainly been concerned with the II–VI compound crystals and at present there is considerable interest in the vacancy centres in CdS, ZnTe and CdTe. There is also interest in the study of ion implantation in the II–VI compounds where, again, the vacancy associated centres are involved [131, 132].

§6. Recombination at deep traps

6.1. *Introduction*

The importance of residual impurities and intrinsic defects on the performance of devices has encouraged considerable effort to characterize and identify the effects of these centres on the electrical and optical properties of the material. These so-called deep traps can act as non-radiative recombination centres or radiative centres in undesired spectral regions and so degrade a light emitting device. But equally important, deep traps can be used to improve material characteristics for device production. For example, carrier lifetime in silicon is controlled by Au and Pt defects while substrate material for microwave devices is produced by adding chromium to GaAs to make it semi-insulating. The most important techniques developed over the past 10 years have been the capacitance methods for determining the trap depths and capture cross-sections. Grimmeiss has reviewed some of these deep-level spectroscopy techniques and results at a recent summer school [133]. As a result of these measurements on Schottky diodes produced from both undoped and doped material the trapping behaviour of many centres is now well characterized. However, the identity or atomic nature of most of these centres is undetermined. Clearly, optical resonance should be able to contribute to these investigations since in the case of radiative centres the energy of emission should be related to the trap depths measured by other methods. My cautiousness in this matter can be understood by considering several preliminary results from a study of GaP epitaxial layers which my laboratory has been carrying out in collaboration with Dr. A.

Peaker and Dr. B. Hamilton (U.M.I.S.T.) and Dr. P. J. Dean (R.S.R.E.): preliminary results of this investigation were given at the second Lund Deep-Level Conference and further details will be published (Killoran *et al.* [134]). Figure 42 shows the results of a comprehensive photocapacitance study of GaP layers diffused with transition metal ions carried out at U.M.I.S.T. and reproduced from Brunwin *et al.* [135]. The levels represent energies at which ions in the reverse biased diodes change charge state and so some care must be exercised in deciding how these levels are related to the various energy levels of the multielection ions of chromium or iron, etc. Our preliminary optical resonance studies on these samples have shown the existence of many magnetic resonance centres but the difficulty in determining the identity of these centres can be illustrated if we consider the example of chromium diffusion into GaP. Two control samples were investigated for both VPE and PLE substrates. The VPE unannealed layer showed a visible luminescence at 540 nm shown in fig. 43 (*a*) which had not previously been discussed in the literature and this emission shows an optical resonance signal similar to that shown in fig. 43 (*a*). When the substrate is annealed at 800°C without chromium diffusion this emission band and the resonance of fig. 45 (*a*) disappear as shown in fig. 43 (*b*) and 44 (*b*). However, when the chromium is introduced by diffusion this emission and associated resonances reappear more strongly than before. The second curve in fig. 43 (*a*) is the spectral dependence of the broad resonance showing that the narrow donor–acceptor bands due to S and C are not involved with the O.D.M.R. signal. The chromium also introduces a very weak emission at 1·1 eV but no resonances have been observed from this emission in these epilayers. The resonance in fig. 44 (*a*) can be decomposed into an electron resonance at $g=1{\cdot}996$, a positive ΔI signal at $g=2{\cdot}05$ with five components in the ratio 1 : 4 : 6 : 4 : 1 typical of a system with $S=\frac{1}{2}$ on a Ga site interacting with four phosphorus neighbours each with nuclear spin $I=\frac{1}{2}$. The line separations give $A_{[100]}=65$ mT. The other two resonances, a three-line spectrum at $g=3{\cdot}9$ and a broad resonance at $g=1{\cdot}96$ are decreases in the luminescence intensity

Fig. 42

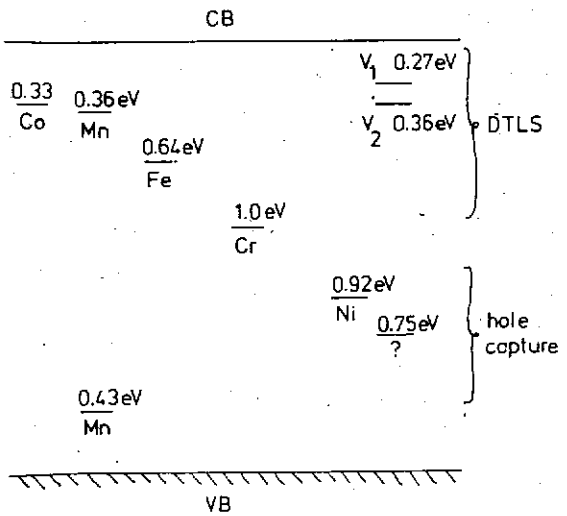

Summary of the photocapacitance investigations of GaP diffused with transition metal ions. (After Brunwin *et al.* [135].)

Fig. 43

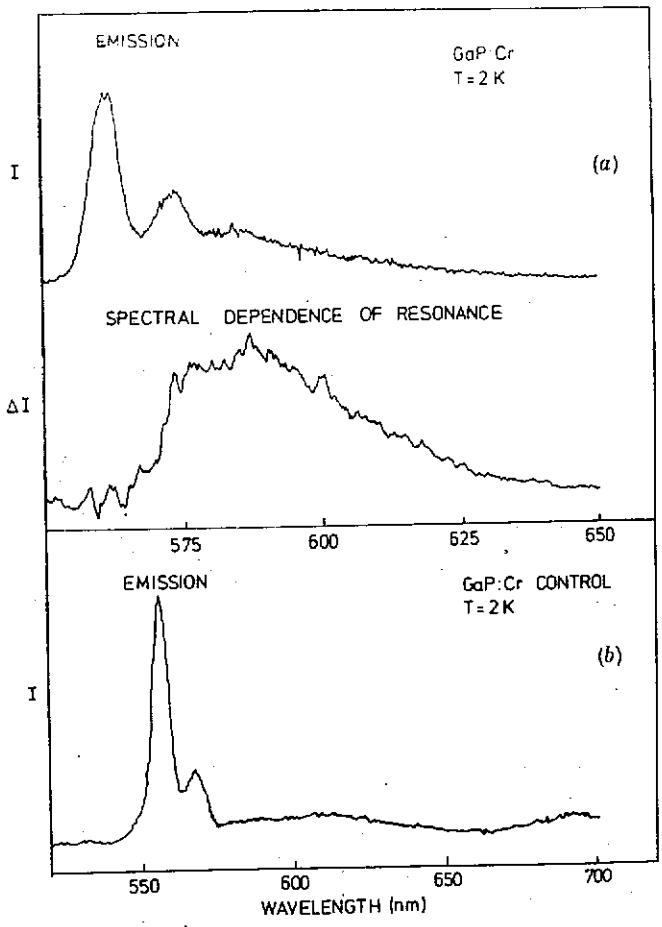

(*a*) Upper curve shows visible emission in the region of S–C pair emission for GaP : Cr material. Lower curve is the spectral dependence of the broad O.D.M.R. signal shown in fig. 44 (*a*). (*b*) Emission spectrum for GaP: control sample where sample was treated by diffusion process without Cr.

at resonance. These signals have been attributed to spin dependent non-radiative processes which compete with the radiative processes and so decrease the luminescence at resonance. For example, the emission at 540 nm may be a donor–acceptor recombination involving a deep acceptor, possibly a Ga-vacancy and so the non-radiative processes would involve donor and transition metal ion resonances related to the tunnelling of an electron to a transition ion instead of recombining radiatively with a hole. These processes are illustrated in fig. 45 where the solid-line transition is the allowed singlet electron–hole radiative recombination path and the dotted line is the allowed non-radiative path. It should be noted that the suggestion that the broad positive five-line O.D.M.R. is due to a V_{Ga} conflicts with the report of Kennedy and Wilsey [136] who report a similar resonance with $g = 2{\cdot}016 \pm 0{\cdot}002$ but a nuclear hyperfine interaction $A_{[100]} = 7$ mT and so clearly a considerable amount of work needs to be done before a better understanding of these defects in GaP is achieved.

Fig. 44

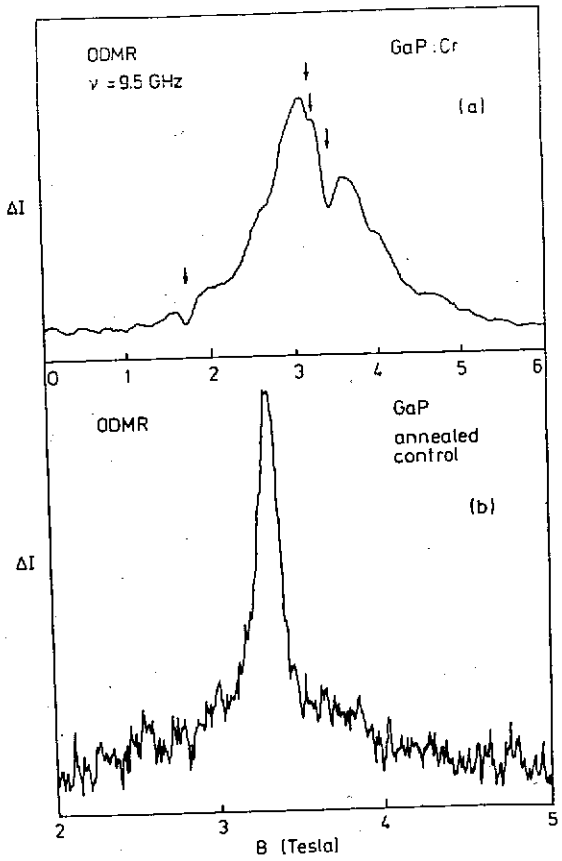

O.D.M.R. signals from emission shown in lower curve of fig. 43 (*a*). The negative signals indicate non-radiative centres. (*b*) Electron and hole resonances observed from the control sample.

Fig. 45

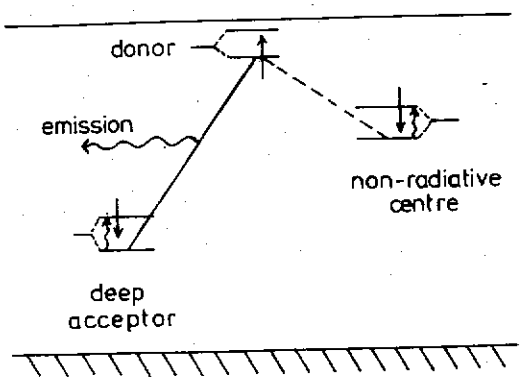

Origin of negative O.D.M.R. signals by resonance at a non-radiative centre coupled to a radiative donor–acceptor process.

Undoubtedly, O.D.M.R. measurements will help with these problems but other experiments such as spin-dependent photoconductivity and spin-dependent photocapacitance studies will be important.

6.2. *GaP : O*

We now turn to a consideration of the role of oxygen in GaP, a problem which has been controversial despite the considerable activity in recent years. It is well established that oxygen produces a deep donor, O^0, in GaP with binding energy of 0·95 eV. This was clearly shown by Dean *et al.* [137] who investigated the near infrared recombination transitions involving O^0 donors and Zn acceptors. Replacing ^{16}O by ^{18}O confirmed the identity of the donor and the binding energy of the single electron was obtained from the transition energies using the donor–acceptor model (eqn. (5.1)). Magnetic resonance of this one electron centre has been reported by Toyotomi and Morigaki [138] and Ill'in *et al.* [139] who observed a broad E.P.R. line at $g = 1{\cdot}996$.

A further comprehensive study was carried out by Dean and Henry [140] in the infrared where an emission with a zero phonon line at 0·841 eV was attributed to a capture process within the one electron oxygen centre. This emission is shown in fig. 47 where the zero-phonon line and lattice and local mode sidebands are indicated. That the emission was due to oxygen was again illustrated by comparing the emission energies of the zero-phonon line and phonon replicas in ^{16}O and ^{18}O doped material. The zero-phonon line shifted 0·7 meV to lower energy in the enriched ^{18}O material. The capture process of the electron can take place between the $1s$(E) and the $1s$(A) states of the donor where the splitting of the ground state arises because of the multivalleyed nature of GaP. Since this transition is strictly forbidden it would be expected that the zero-phonon emission would be weak and, in fact, this is observed to be the case. In order to strengthen this assignment of the 0·841 eV emission to the O^0 centre Dean and Henry [140] measured the excitation spectrum of the emission and attributed the observed excitation lines to transitions within the one-electron energy scheme. Despite this firm evidence that the 0·841 eV emission is the capture luminescence within the O^0 donor, the assignment was not unanimously accepted. For example, Morgan [141] compared the phonon energies of the near infrared donor–acceptor transitions as measured by Monemar and Samuelson [142] with the phonon structure observed in the 0·841 eV emission and showed that there

Fig. 46

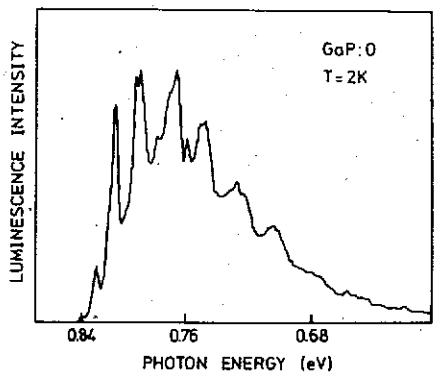

Infrared emission with no-phonon line at 0·841 eV for GaP : O.

Fig. 47

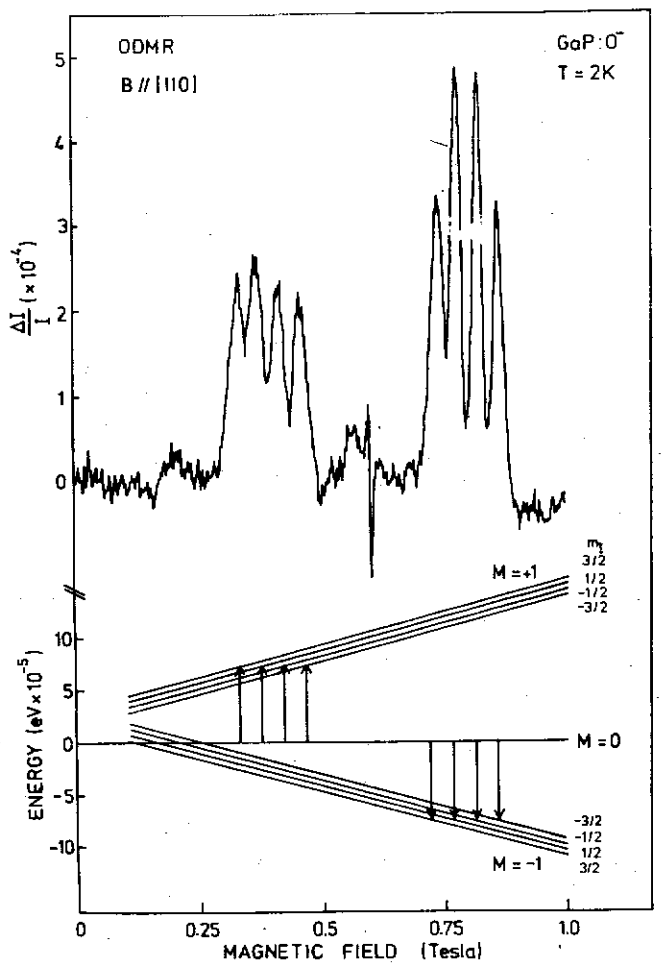

Upper curve is O.D.M.R. signal observed from emission shown in fig. 46. Lower curve shows triplet level scheme for the O^- centre where the hyperfine interaction is with one Ga nucleus.

were considerable differences. He concluded that this emission was related to a capture process within the two electron oxygen centre, O^-, which was known to exist from photocapacitance and photoconductivity studies by Kukimoto *et al.* [143], Henry *et al.* [144] and Grimmeiss *et al.* [145]. These measurements had shown that a second electron can be bound at the O^0 centre with binding energy approximately equal to the first electron. In fact, Dean and Henry [140] had investigated the effects of increasing the Zn acceptor concentration on the intensities of the two emissions and the optical saturation behaviour at high excitation powers. In the first experiment the donor–acceptor emission increased but the 0·839 eV emission was quenched while in the second experiment the donor–acceptor emission saturated but the 0·841 eV emission did not. Both these results were surprising in view of the strength of the evidence for the O^0 capture model and although these authors proposed possible Auger processes to explain these results, undoubtedly, an explanation in terms of the 0·841 eV emission being due to O^- was attractive.

Gal *et al.* [146] investigated the 0·841 eV emission by O.D.M.R. using the 799 nm krypton line to avoid excitation of the donor–acceptor emission. At 16·5 GHz the resonances shown in the upper part of fig. 47 were obtained for $B\|[110]$. The resonances are characteristic of a spin–triplet system in axial symmetry where the electrons interact strongly with one Ga neighbour. The hamiltonian for such a system is

$$\mathscr{H}=g_{\|}\mu_B B_z S_z+g_{\perp}\mu_B(B_x S_x+B_y S_y)+D[S_z-\tfrac{1}{3}S(S+1)]+A_1\mathbf{I}\cdot\mathbf{S}+A_2\mathbf{I}\cdot\mathbf{S},$$

where $S=1$, $g_{\|}=2{\cdot}011\pm0{\cdot}005$, $D=+2{\cdot}32\pm0{\cdot}01\times10^{-5}$ eV and the hyperfine interaction has two components, $A_1=4{\cdot}40\pm0{\cdot}02\times10^{-6}$ eV, $A_2=5{\cdot}88\pm0{\cdot}02\times10^{-6}$ eV due to the two isotopes ^{69}Ga and ^{71}Ga which occur in the abundance ratio of 60 : 40. (In fact the O.D.M.R. spectra in fig. 47 can easily be seen to consist of eight lines at high resolution). The energy level scheme and the transitions for one Ga isotope are shown in the lower part of fig. 47. The zero field splitting, D, arises from the [110] distortion of the centre which allows the O^- centre to interact strongly with one Ga atom and not equally with the four which surround an ion on a phosphorus site. Both of the resonances in fig. 47 are increases in the emission intensity corresponding to an unthermalized system where the population differences between the $|\pm1\rangle$ and $|0\rangle$ states are determined by the different decay rates. For $B\|[110]$ the populations of the $|\pm1\rangle$ states drop below that of the $|0\rangle$ state. At resonance the transitions $|0\rangle\rightarrow|\pm1\rangle$ increase the emission intensity. The sign of D as positive was determined by observing the emission with a circular polarizer. The low-field resonance corresponds to σ^+ and the high field to σ^-. One important test of an unthermalized triplet system is the observation of a level crossing signal as either the circular polarization or the emission intensity is measured as a function of magnetic field. As the $|-1\rangle$ state crosses the $|0\rangle$ state the two states are mixed and the emission intensity increases.

If the exciton and donor–acceptor emissions are excited with an argon ion laser. the triplet O.D.M.R. described above are observed as an increase in intensity on the infrared donor–acceptor transitions and as a decrease of the bound exciton emission. This was explained by the proposal that at resonance the number of O^- centres in the ground state increased and the formation of O^0 centres by hole capture from acceptors also increased. This decrease in the number of neutral acceptors at resonance produced a corresponding decrease in the (A^0, X) recombination. The important question is therefore whether one can be sure that the resonance originates from the 0·841 eV emission. The sign of the O.D.M.R. signal, the strong polarization dependences of the resonances and the strong level crossing observed when monitoring the 0·839 eV emission were strong evidence for the correctness of the assignment of this band to O^- but the reasonable degree of uncertainty allowed the controversy to continue.

A further and perhaps final episode to this story has recently been published by Gal *et al.* [147] who undertook a series of measurements on the zero phonon emission using a very sensitive Ge detector (North Coast). It was expected that Zeeman measurements would resolve the controversy and, in fact, the no-phonon line split into three in a magnetic field. However, the results could be explained by either the O^0 or O^- capture models. Stress measurements finally resolved the matter since for stress along [111] the no-phonon line did not split while for stress along [110] and [100] the line split into two components in both cases. The results show that the centre has [100] symmetry as expected for the $1s$(E) state of O^0 since this state is generated from the valley orbit splitting with [100] symmetry. The O.D.M.R. results

of Gal *et al.* [146] were reinterpreted in terms of a model involving a spin-conserving Auger process which allowed the memory of the populations of the triplet system (O^-) to be conserved and observable via the $1s(E) \rightarrow 1s(A)$ emission. This model is shown in fig. 48 where the triplet O^- state is shown breaking up by an Auger process where one electron recombines with a hole at an acceptor and the second electron is left in the $1s(E)$ state of O^0. The populations of this state are determined by spin memory of the O^- states and so resonance in the triplet can be observed on the O^0 capture luminescence.

Fig. 48

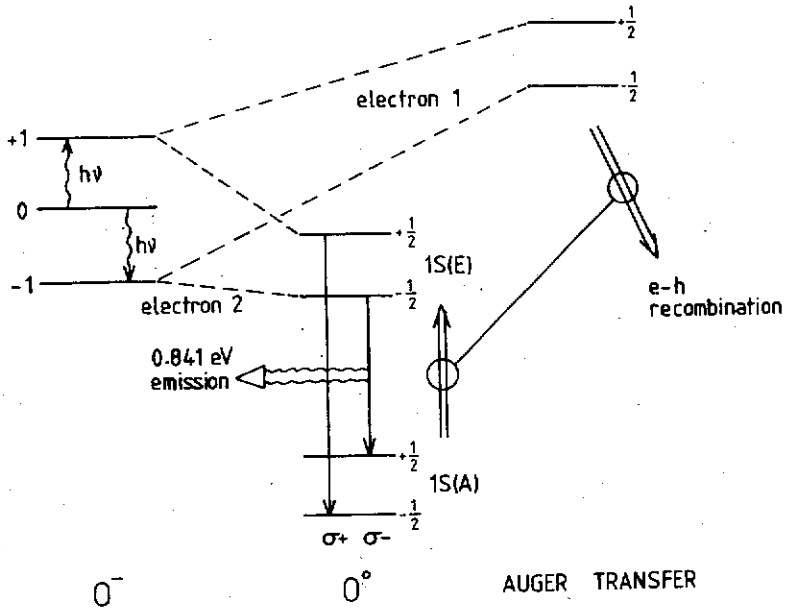

Spin dependent Auger model showing how triplet O^- O.D.M.R. can be observed on the O^0 singlet emission. The O^- decays leaving the O^0 centre in the excited state with populations related to the O^- state.

6.3. *GaAs : Cr*

The final problem that I would like to discuss briefly is that of the infrared emission of GaAs : Cr, the semi-insulating material used as substrates for microwave FETs. This material has been basic to the technology of solid state devices but the role of chromium ions as electron and hole traps is not well understood despite many investigations in recent years. The 0·839 eV emission was first reported by Koschel *et al.* [148] and Stocker and Schmidt [149] and investigated by Lightowlers and Penchina [150] and Lightowlers *et al.* [151] who showed that both in absorption and emission the zero phonon line consisted of many components, up to 13 depending on the temperature. It has been difficult to reconcile the multistructured zero phonon emission with a model based on transitions within a Jahn–Teller distorted Cr^{2+} ion such as that discussed by Krebs and Stauss [152]. These authors have carried out a comprehensive E.P.R. investigation of the Cr^{1+}, Cr^{2+} and Cr^{3+} ions in GaAs and, in particular, have shown that the ground state of Cr^{2+} is well described by a [100] static Jahn–Teller distorted ion. Stress measurements by Krebs and Stauss [153] and infrared E.P.R. studies by Wagner and White [154] have confirmed this assignment.

Thus, despite the quite certain occurrence of Cr^{2+} as the dominant charge state in semi-insulating GaAs the static model could not account for the number of lines observed in the absorption and luminescence measurements.

White [155] was the first to analyse in detail the information about GaAs : Cr and, drawing a parallel between the characteristic emission of excitons at isoelectronic traps and the form of the 0·839 eV, he suggested that this emission is due to electron–hole recombination at a nearest neighbour (Cr^{2+}–D^{+}) pair. The symmetry of such a centre would be axial along [111]. Recently, O.D.M.R. measurements by Killoran *et al.* [156] and Zeeman studies by Killoran *et al.* [156, 157] and Eaves *et al.* [158] have, in fact, shown that the 0·839 eV emission is from a centre with such symmetry. The O.D.M.R. signals for $B\|[100]$ have already been given in fig. 11 and the two strongest lines have been investigated in detail. The line at 0·20 T splits into three lines as the magnetic field is rotated away from [100] in the (110) plane as shown in fig. 49. This splitting can be analysed in terms of a centre with orthorhombic symmetry with g values $g_1 = 2{\cdot}13 \pm 0{\cdot}05$, $g_2 = 3{\cdot}50 \pm 0{\cdot}09$ and $g_3 = 3{\cdot}78 \pm 0{\cdot}02$ where the principal distortion is along [111]. The observed symmetry of this excited state is consistent with the Zeeman measurements on the zero-phonon line where the angular dependence measurements are best fitted to a centre with a small orthorhombic distortion [157]. At present attempts are being made to link the excited state g-values known from O.D.M.R. to the Zeeman measurements which involve both excited and ground state g-values. The results so far are consistent with the White [155] model but may be explained by a dynamic Jahn–Teller effect on the

Fig. 49

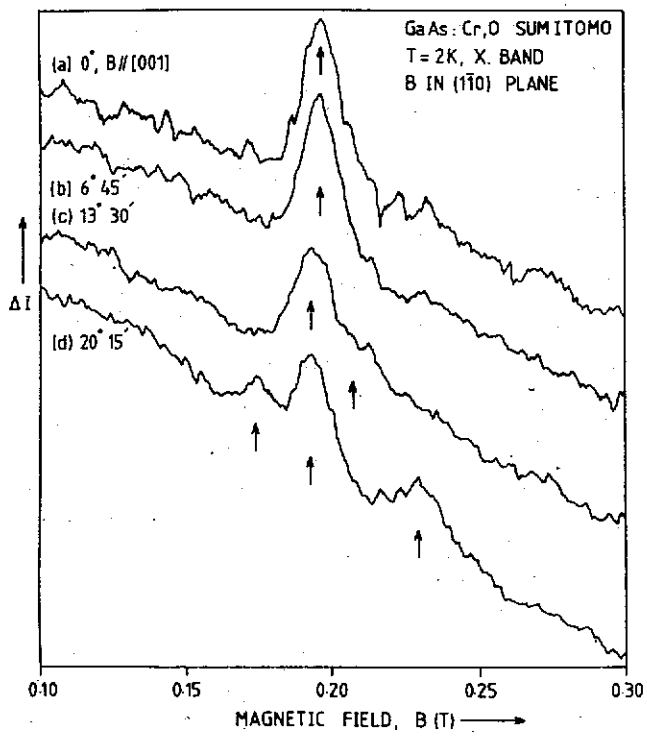

Angular dependence in the (110) plane for the GaAs : Cr O.D.M.R. signal at 0·20 T for $B\|[001]$.

Fig. 50

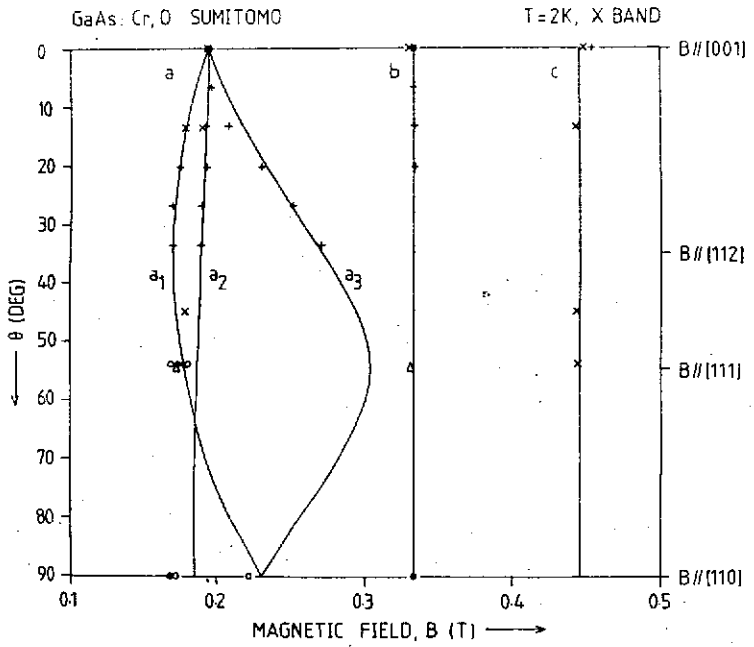

Plot of O.D.M.R. signals for GaAs : Cr for rotation of the magnetic field in the (110) plane. The low-field resonance (*a*) is as shown in fig. 49.

levels of Cr^{2+}. Lowther [159] showed that such a model could generate sufficient number of levels to explain the optical data, though in this case a [100] distortion was considered. Recently, Bates *et al.* [160] and Voillot *et al.* [161] have interpreted the optical data by considering an isolated Cr^{2+} ion with C_{3v} Jahn–Teller distortion. The conclusion from these investigations is clearly that the E.P.R. of Cr^{2+} with [100] symmetry measured by Krebs and Stauss [152] is not the ground state of the centre giving the 0·839 eV emission. In fact, Clerjaud *et al.* [162] has recently observed several absorptions near 6600 cm^{-1} which correlate well with the tetragonal Cr^{2+} model.

6.4. *Conclusions*

The investigations of deep traps by O.D.M.R. and by absorption resonance experiments is in a very early stage and clearly has an exciting future. Current studies are being directed to correlation of resonances observed by the optical methods with those detected via the transport properties and undoubtedly investigations of deep levels in silicon by photoconductivity detected resonances is going to be important. Preliminary attempts to detect resonances via the capacitance in a Schottky diode have been encouraging but so far unambiguous results on a sample well characterized by DLTS have not been obtained but success would give a new dimension to these studies of spin effects in semiconductors.

§7. Recombination processes in amorphous semiconductors

7.1. *Introduction*

The development of the application of O.D.M.R. to semiconductors has principally taken place via studies of crystalline material where, in particular,

exciton and donor–acceptor recombination processes are well understood. The extension to the study of amorphous semiconductors was a natural consequence of the potential for O.D.M.R. to identify defects associated with recombination processes. The importance of conventional E.P.R. in the field of glassy and amorphous materials should also be noted and comprehensive studies using photoexcitation of samples such as chalcogenide glasses and a-Si : H have provided valuable information on structural defects [20, 21]. Unfortunately, these structural defects all have resonances near $g=2$ and so the importance of the studies lies in correlation of the magnetic resonance data with preparation procedures, excitation radiation and annealing behaviour. Two systems have been studied in some detail by O.D.M.R. These are the glass chalcogenides As_2Se_3 and As_2S_3 with parallel studies of crystalline material and the technologically important a-Si : H; in the following sections these results are discussed in detail.

7.2. *As_2Se_3 and As_2S_3*

The emissions from crystalline and amorphous As_2Se_3 and As_2S_3 at low temperatures are remarkably similar with broad bands occurring at midband gap with energies 0·9 eV and 2·0 eV, respectively. Despite many detailed investigations of these emissions the nature of the defects involved in the recombination processes has not been clarified. Mott *et al.* [163] have suggested that in the case of these glasses the diamagnetic D^+ and D^- centres are important to explain the lack of magnetic resonance observations in these materials. Bishop *et al.* [20] have carried out a comprehensive investigation of photoinduced E.S.R. in As_2Se_3 and attributed the signals to holes trapped on Se ions and electrons trapped at As sites. In the latter case a hyperfine interaction with the As nuclear spins provided a satisfactory explanation for the E.S.R. line shape. More recently, Biegelsen and Street [164] re-examined the photoinduced signals at 30 K and showed signals with approximately two orders of magnitude in spin density (up to 10^{20}) than previous measurements. Annealing behaviour showed fast and slow processes, the former being related to the signals observed by Bishop *et al.* [20] and the latter to new photostructural defects involved in the fatigue process as non-radiative centres. See also Mollot *et al.* [165] for a discussion of high-spin densities at 77 K and PL fatigue processes in chalcogenide glasses. A general discussion of the defects in these materials can be found in the review by Davis [166]. In contrast with the glasses no photoinduced or dark E.S.R. has been observed in crystals of these materials.

Suzuki *et al.* [167] were the first to observe O.D.M.R. in a-As_2S_3 and at 23 GHz observed a broad line with a 0·12 T half-width. It was not possible to identify the centres involved in the recombination process. The broad O.D.M.R. signal is most likely to be a composite signal.

In the case of a-As_2Se_3 a similar broad O.D.M.R. signal centred at $g=2·0$ was observed by Depinna *et al.* [168] and is illustrated in fig. 51. The line shape was little affected by doping either with Cu or Ge and the line width was measured to be 90 mT. In the case of undoped crystalline As_2Se_3 a broad resonance was also observed by O.D.M.R., though this was much weaker than for the case of a-As_2Se_3. However, in Ge doped crystalline As_2Se_3 several signals were observed as illustrated in the lower part of fig. 52. In the upper part of the figure the O.D.M.R. signal has been analysed in terms of three overlapping resonances; a narrow resonance at $g=2·1$, a four-line spectrum with $g=2·0$ and $A=11$ mT corresponding to interaction arsenic nuclei with $I=\frac{3}{2}$ and a broad (50 mT) resonance at $g=2·05$. A spectral dependence measurement

Fig. 51

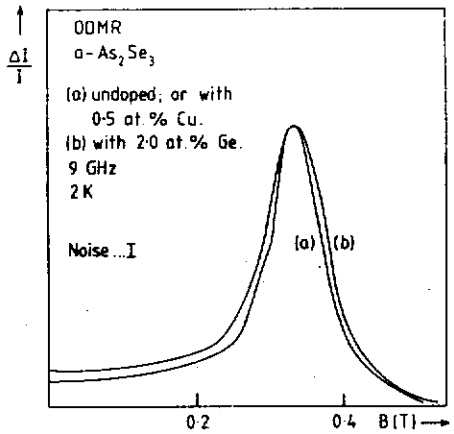

Broad O.D.M.R. signals in undoped and Ge doped a-As_2Se_3.

Fig. 52

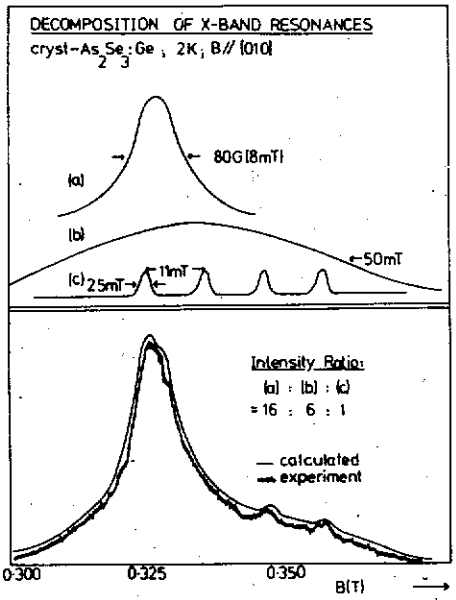

Lower curve shows the experimental O.D.M.R. signal for Ge-doped crystalline As_2Se_3 and signal calculated from the three resonances shown in upper curve.

was carried out on the maximum of the O.D.M.R. signal and it was clear that at least two distinct emission processes, one at 1·12 eV and the other at 0·8 eV. The importance of the Ge doping was explained in terms of the formation of valence alternation pairs such as that illustrated in fig. 53, where the Ge has substituted at an As and taken four-fold coordination (fig. 53 (*b*)). In this model the O.D.M.R. signal consisting of four hyperfine lines is the result of an electron localized on one As atom; this is in contrast to the signals observed by Bishop *et al.* [20] where the optically induced E.S.R. in the amorphous material is due to interaction with two As nuclei.

Fig. 53

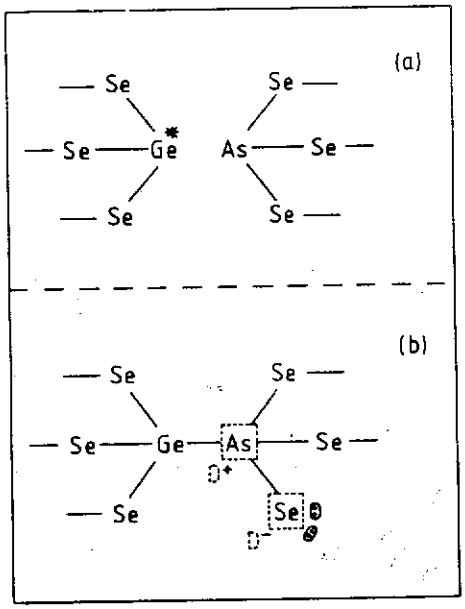

Possible production of I.V.A.P.s in c-As_2Se_3 through Ge doping; (a) Ge with dangling bond, (b) I.V.A.P.

In the As_2Se_3 : Ge crystals the nearest As site is occupied by a Ge atom which has small nuclear spin abundance. The narrow resonance at $g=2{\cdot}1$ has been assigned to the hole on a chalcogenide atom. The recombination process was attributed to electrons and holes localized at weakly coupled D^+ and D^- centres in analogy with donor–acceptor pair recombination in II–VI compounds discussed in §5. The resonances were reported by Depinna *et al.* [168] as increases in the luminescence but have more recently been shown by the same authors to be decreases in emission implying that the defects act as non-radiative centres, perhaps related to the defects reported by Biegelsen and Street [164] which were also attributed to non-radiative processes.

7.3. *a-Si : H*

The device potential of hydrogenated amorphous silicon has encouraged a wide range of investigations of this material. In particular, the optical properties have been studied in detail by Street *et al.* [169], Nashashibi *et al.* [170], Paesler and Paul [171], Pankove and Carlson [172] and Austin *et al.* [173]. There are two methods of preparation, the most common being the glow–discharge (gd) deposition of films from a silane–argon gas mixture but the sputtering (sp) of films in a hydrogen atmosphere is also important. For both gd and sp a-Si : H, it is accepted that high luminescence quantum efficiency corresponds to a low density of dangling bonds which can be monitored by E.S.R. and give a resonance $g=2{\cdot}0055$ (Brodsky *et al.* [174]). Thus the idea that dangling bonds act as non-radiative recombination centres is well established.

Optically detected magnetic resonance in gd a-Si : H was independently investigated by Morigaki *et al.* [175], Biegelsen *et al.* [176] and Lampel and Solomon

[177]. This original work was all carried out using photodetectors sensitive to energies greater than 1·1 eV, i.e. the high-energy part of the emission. Both positive and negative signals were observed and, in particular Morigaki *et al.* [175] introduced the idea that the positive signals are related to weakly coupled donor–acceptor pairs with the negative signals D_1 and D_2 due to non-radiative processes such as those discussed for crystalline material in § 7·1. Biegelsen *et al.* [176] observed only one negative signal at low microwave chopping frequencies which became a positive signal at high frequencies. A recent O.D.M.R. study of both gd and sp a-Si : H by Depinna *et al.* [178] using a Ge-detector which covers an energy range extending from 0·7–1·8 eV has resolved the inconsistencies between the initial reports. The results of the study showed that the emission from a-Si : H, irrespective of preparation method, is not a single emission band but consists of three distinct bands centred near 1·4 eV, 1·25 eV and 0·9 eV. For example, fig. 54 (*a*) shows the emission from a sputtered a-Si sample excited with 2·41 eV radiation. The major O.D.M.R. signals obtained using the Ge detector are illustrated in fig. 55 (*a*) and (*b*) where it can be seen that a strong quenching resonance (Q) at $g = 2{\cdot}005$ is observed when the short wavelength (1·55 eV) of the band is monitored while at longer wavelengths (~0·9 eV) an enhancing resonance (E_1) at $g = 2{\cdot}007$ is observed. Spectral dependences of these resonances are shown in fig. 54 (*b*) and (*c*) respectively. These two signals were observed in a wide range of samples prepared by both gd and sp material and the

Fig. 54

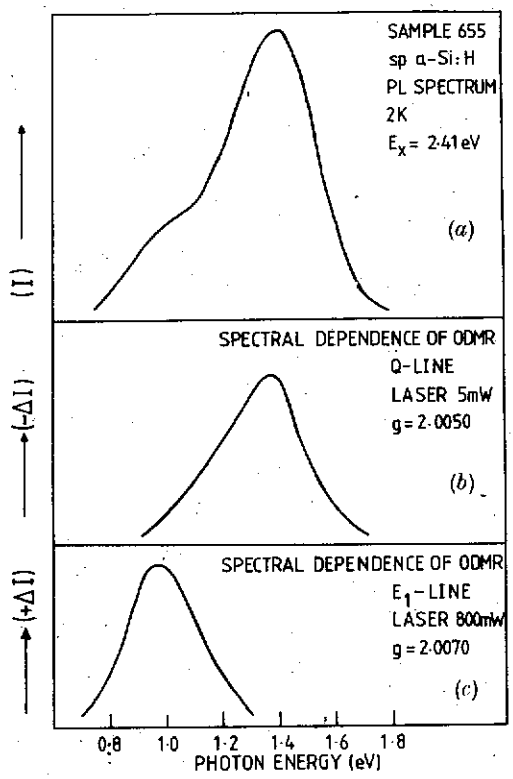

(*a*) Emission spectrum for a sputtered *a*-Si : H sample prepared at 200°C showing 0·9 eV emission. (*b*) Spectral dependences of Q line shown in fig. 55. (*c*) Spectral dependence of E_1 line shown in fig. 55.

Fig. 55

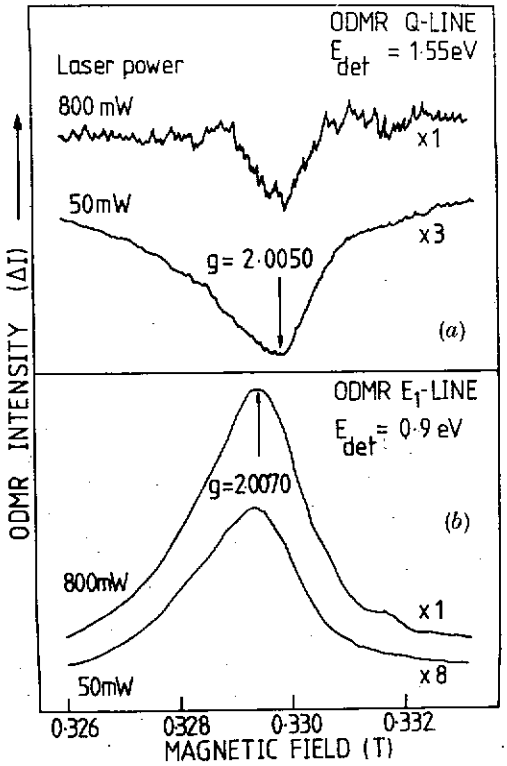

(*a*) O.D.M.R. signal obtained for two laser powers, 50 mW and 800 mW. The signal is a decrease in the emission at 1·55 eV and is labelled the Q resonance. (*b*) O.D.M.R. signal for emission at 0·9 eV, again for two laser powers. The resonance is an increase in intensity and is labelled E_1.

strengths of the resonances were strongly dependent on laser and microwave power. In some materials showing the 1·25 eV emission a broad enhancing resonance (E_2 with $g=2{\cdot}00$, $B=10$–20 mT) is observed. Also in this spectral region a third enhancing resonance (E_3) which overlaps E_2 can sometimes be observed.

Thus the results of Morigaki *et al.* [175] must be reinterpreted since D_1 and D_2 result from Q and E_1 and the suggestion by Movaghar *et al.* [179] that the sign reversal of the Biegelsen *et al.* [176] O.D.M.R. signals was the result of different detection frequencies is not necessary since these signals come from different spectral regions. (It does not, however, rule out the possibility of such a reversal under suitable conditions).

Depinna *et al.* [178] also investigated the waveform of the Q and E_1 signals showing that a donor–acceptor model along the lines of the proposals by Morigaki *et al.* [175] is appropriate. The suggestion by Biegelsen *et al.* [176] that the resonances arise for a geminate pair model could not be substantiated. The quenching (Q) resonance can be deconvolved into two lines, one with $g=2{\cdot}0045$, $B_{\mathrm{FWHM}}=0{\cdot}5$ mT and another near $g=2{\cdot}01$, $B_{\mathrm{FWHM}}=2$ mT as shown in fig. 56. These signals correlate with the observed L.E.S.R. observed by Friedrich and Kaplan [180] and Street [181]. Thus the Q resonances are attributed to a non-radiative process, mainly coupled to the high-energy side of the photoluminescence. This process is shown in

Fig. 56

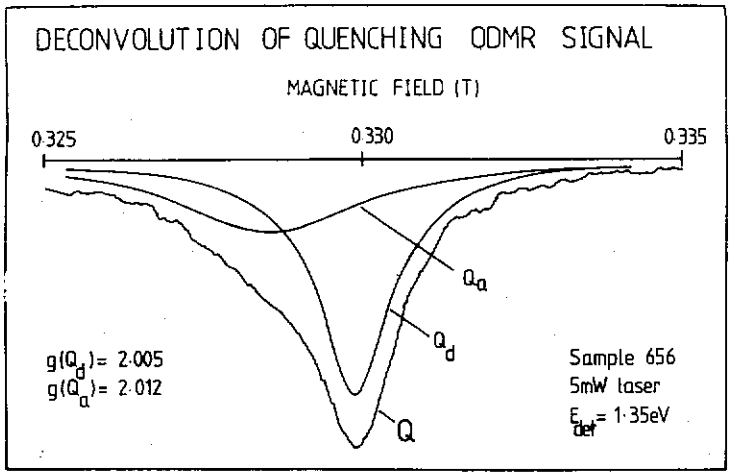

Proposed energy scheme for defects observed by O.D.M.R. in *a*-Si : H. Labels correspond to signals observed by Depinna *et al.* (1981); d = donor and a = acceptor.

fig. 57 as the dashed transitions. The resonance E_1 is assigned to a radiative donor–acceptor pair transition and can be deconvolved into two lines $g = 2·006$ and $g = 2·01$. These two signals are observed on the 0·9 eV emission but the $g = 2·01$ component disappears on the 1·25 eV emission and a broad line (~20 mT wide) is observed instead. The $g = 2·01$ component is probably the same centre associated with the Q-resonance and the narrow $g = 2·006$ component is close to the dangling bond g-value suggesting that a radiative dangling bond may well be the electron centre in the 0·9 eV emission. Such a suggestion was also proposed by Street [181] who envisaged the dangling bond as a non-radiative centre with a small allowed radiative probability. The O.D.M.R. results of Depinna *et al.* [178] suggest that the $g = 2·006$ centre responsible for the 0·9 eV emission is also responsible for the 1·25 eV emission which forms the main constituent of the P.L. in the highest quantum efficiency glow discharge samples.

Fig. 57

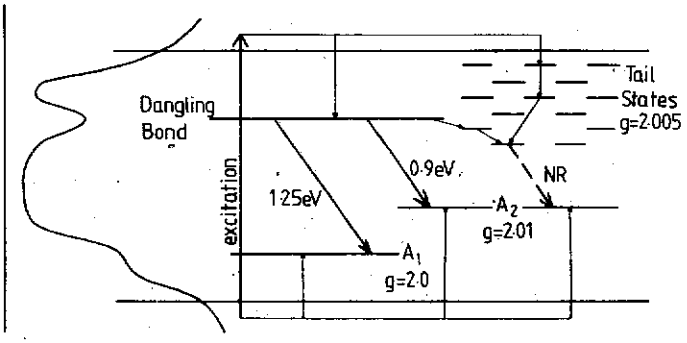

A possible model for recombination in a-Si : H involving radiative dangling bonds for the 1·25 eV and 0·9 eV emissions.

Figure 57 summarizes the results of Depinna *et al.* [178]. The three bands of distinct origin are observable in all samples. The 0·9 eV band is usually observed as a well-resolved emission whereas the 1·4 eV and 1·25 eV bands merge, though the intensities do not correlate so they are independent processes, possibly excitonic like at the highest energy and donor–acceptor pair like at lower energies. The strengths of these bands depend on the preparation conditions. The authors have proposed that the dangling bond is the radiative electron centre for both the 0·9 eV and 1·25 eV bands and have shown [182] that the recombination process can be described in detail by the pair model developed for crystalline donor–acceptor recombination [105]. (A similar pair model has been published by Kaplan *et al.* [183].)

§ 8. Summary

The investigation of recombination processes in semiconductors by O.D.M.R. is very much an on-going subject with many new and exciting results being reported as more groups become involved in this work. For example, Lee *et al.* [184] have recently observed triplet exciton recombination in 6H SiC with titanium which acts as an isoelectronic impurity. Remarkably sharp line resonances and level crossings were observed with structure which was related to the different titanium nuclear isotopes ^{46}Ti to ^{50}Ti. The origin of this effect has been attributed to an isotope effect on the zero-field splitting D. Similar, previously unidentified, structure in the level crossing of bound excitons in GaSe most probably has the same origin [66]. Triplet exciton recombination has also been investigated in GaP : Cu and GaP : Cu,Li. The addition of Cu produces emissions at 2·177 eV and 1·91 eV. O.D.M.R. from the latter luminescence shows a triplet exciton spectra characteristic of recombination at a [100] defect which has been attributed to Cu_{Ga}—Cu_I pairs [185]. The 2·175 eV emissions and the effect of adding Li which quenches this luminescence and produces a very complicated spectrum with many sharp lines is currently under investigation. Triplet excitons have also been observed in HgI_2 [186] and PbI_2[187]. The role of Cu in II–VI compounds has been a matter of controversy for many years. An investigation of O.D.M.R. signals in ZnSe fired in Zn : Cu alloy has shown that Cu_{Zn} acts primarily as a non-radiative path for the copper red luminescence. Copper associated centres related to the copper green and red luminescences were observed directly in the visible and indirectly as negative signals in the infrared [188]. A detailed study of O.D.M.R. signals from the Cu–infrared luminescence in ZnS is also underway at present [189]. This follows a study of ZnS : Sc, Cr where the recombination involving Sc donors and (V_{Zn}–Sc) acceptors has been investigated by O.D.M.R. and the important technique of monitoring the strength of the Cr^+ E.P.R. signal to determine electron and hole ionization energies [190].

The important challenges for the future are the identification of defects, particularly vacancy associated centres, in GaAs, GaP, InP and Si.

Acknowledgments

Many collaborators must be thanked for their contributions to the studies reported in this paper. I am grateful to J. J. Davies, J. E. Nicholls, D. J. Dunstan, N. Killoran, P. Dawson, S. Depinna, W. E. Lamb, M. Godlewski, J. R. James, W. E. Hagston, M. Gal, P. J. Dean, B. Monemar, E. C. Lightowlers, M. O. Henry, K. Morigaki, G. Lampel, C. Weisbuch, C. Hermann, D. Paget, A. Nakamura, R. Cox, G. D. Watkins and to many others who have encouraged these investigations. I am

indebted to G. Sowersby and E. Norman for their excellent technical assistance without which this work would not have been possible.

These investigations have been generously supported by grants from the Science Research Council, The Royal Society and the Ministry of Defence.

References

[1] Geschwind, S., Collins, R. J., and Schawlow, A. L., 1959, *Phys. Rev. Lett.*, **3**, 545.
[2] Geschwind, S., Collins, R. J., Cohen, R. L., and Chinn, S. R., 1967, *Phys. Rev.*, **137**, 1087.
[3] Geschwind, S., 1972. *Electron Paramagnetic Resonance* (New York: Plenum). Chap. 5.
[4] Henderson, B., 1978. *Semicond. Insulators*, **3**, 299.
[5] Zakharchenya, B. P., 1972, *Proceedings of the International Conference on Physics of Semiconductors*, Warsaw, edited by M. Miasek (Amsterdam: Elsevier), p. 1315.
[6] Zakharchenya, B. P., 1978. *Proceedings of the Specialized Colloque Ampere, Dublin. Semicond. Insul.*, **4**, 35. (This conference proceedings covers a wide variety of organic, inorganic and semiconductor optical resonance studies and is a very useful general reference.)
[7] Zakharchenya, B. P., 1979, *Proceedings of the International Conference on Physics of Semiconductors*, Edinburgh, edited by B. L. H. Wilson (London: Institute of Physics), p. 31.
[8] Lampel, G., 1974, *Proceedings of the International Conference on Physics of Semiconductors*, Stuttgart, edited by M. H. Pilkuhn (Stuttgart: Teubner), p. 743.
[9] Planel, R., 1978. *Proceedings of the International Conference on Recombination in Semiconductors*, Southampton. *Solid-St. Electron.*, **21**, 1437.
[10] Davies, J. J., 1976, *Contemp. Phys.*, **17**, 275.
[11] Davies, J. J., Nicholls, J. E., and Cavenett, B. C., 1978, *Semicond. Insul.*, **4**, 101.
[12] Cavenett, B. C., 1978, *Luminescence Spectroscopy*, edited by M. D. Lumb (New York: Academic Press), Chap. 5.
[13] Cavenett, B. C., 1979, *Proceedings of the International Conference on Luminescence*, Paris, *J. Lumin.*, **18/19**, 846.
[14] Cavenett, B. C., 1980, *Proceedings of the International Conference on Semiconductors, Kyoto, 1980, J. phys. Soc. Japan*, **49**, Suppl. A. 611.
[15] Ludwig, G. W., and Woodbury, H. H., 1962, *Solid St. Phys.*, **13**, 223.
[16] Title, R. S., 1967, *Physics and Chemistry of II–VI Compounds*, edited by M. Aven and J. S. Prener (Amsterdam: North Holland). Chap. 6.
[17] Lancaster, G., 1967. *Electron Spin Resonance in Semiconductors* (New York: Plenum).
[18] Varshni, Y. P., 1967 a, *Phys. Stat. Sol.*, **19**, 459; 1967 b, *Ibid.*, **20**, 9.
[19] Schneider, J., 1967, *II–VI Semiconducting Compounds*, edited by D. G. Thomas (New York: Benjamin), p. 40.
[20] Bishop, S. G., Strom, U., and Taylor, P. C., 1977, *Phys. Rev.* B, **15**, 2278.
[21] Solomon, I., 1979, *Amorphous Semiconductors*, in *Topics in Applied Physics*, Vol. 36, edited by M. H. Brodsky (New York: Springer-Verlag).
[22] Morigaki, K., 1978, *Institute of Physics Conference Series, No. 43*, edited by B. L. H. Wilson, p. 943.
[23] Kaufmann, U., and Schneider, J., 1980, *Adv. Solid St. Phys.*, **20**, 87 (Vieweg 1980). (New York: Academic Press); p. 97.
[24] Watkins, G., 1965, *Radiation Damage in Semiconductors* (New York: Academic Press), p. 97.
[25] Abragam, A., and Bleaney, B., 1976, *Electron Paramagnetic Resonance of Transition Ions* (Oxford: Clarendon Press).
[26] Poole, C. P., 1967, *Electron Spin Resonance* (Wiley).
[27] Dawson, P., Dunstan, D. J., and Cavenett, B. C., 1978, *Semicond. Insul.*, **4**, 91.
[28] Luttinger, J. M., 1956, *Phys. Rev.*, **102**, 1030.
[29] Yafet, Y., and Thomas, D. G., 1963, *Phys. Rev.*, **131**, 2405.
[30] Zeiger, H. J., and Pratt, G. W., 1973, *Magnetic Interactions in Solids* (Oxford).
[31] Kemp, J. C., Zinaker, W. M., Glaze, J. A., and Cheng, J. C., 1968, *Phy. Rev.*, **171**, 1024.

[32] ROMESTAIN, R., GESCHWIND, S., and DEVLIN, G. E., 1974, *Phys. Rev. Lett.*, **33**, 10.
[33] ROMESTAIN, R., 1980, *J. Phys.* C, **13**, 1097.
[34] SOLOMON, I., 1972, *Proceedings of the International Conference on Physics of Semiconductors*, Warsaw, edited by M. Miasek (Amsterdam: Elsevier), p. 27.
[35] CHAGALVIEL, J. N., 1975, *Phys. Rev.* B, **11**, 3918.
[36] LEPINE, D. J., 1972, *Phys. Rev.*, **6**, 436.
[37] MAXWELL, R., and HONIG, A., 1966, *Phys. Rev. Lett.*, **17**, L525.
[38] MORIGAKI, K., and ONA, M., 1974, *J. phys. Soc. Japan*, **36**, 1049.
[39] CAVENETT, B. C., and BRUNWIN, R. F., 1976, *Proceedings of the International Conference on Physics of Semiconductors*, Rome, edited by F. G. Fumi, p. 1016.
[40] MENDZ, G., and HANEMAN, D., 1980, *J. Phys.* C, **13**, 6737.
[41] CAVENETT, B. C., *Progress in Crystal Growth and Characterization* (to be published).
[42] HERMANN, C., 1977, *Annls Phys.*, **2**, 5.
[43] PARSONS, R. R., 1969, *Phys. Rev. Lett.*, **23**, 1152.
[44] HERMANN, C., and LAMPEL, G., *Phys. Rev. Lett.*, **27**, 373.
[45] WEISBUCH, C., and HERMANN, C., 1977, *Phys. Rev.* B, **15**, 816.
[46] CAVENETT, B. C., HERMANN, C., LAMPEL, G., NAKAMURA, A., PAGET, D., and WEISBUCH, C., 1978, *Semicond. Insul.*, **4**, 81.
[47] NAKAMURA, A., PAGET, D., HERMANN, C., WEISBUCH, C., LAMPEL, G., and CAVENETT, B. C., 1979, *Solid St. Commun.*, **30**, 411.
[48] WEISBUCH, C., 1976, *Proc. Colloque Ampere, Heidelberg, Magnetic Resonance and Related Phenomena*, edited by H. Brunner, p. 293.
[49] LOOK, D. C., and MOORE, D. L., 1972, *Phys. Rev.* B, **5**, 3406.
[50] WALKER, T. W., LITTON, C. W., REYNOLDS, D. C., COLLINS, T. C., WALLACE, W. A., GORRELL, J. H., and JUNGLING, K. C., 1972, *Proceedings of the International Conference on Physics of Semiconductors*, Warsaw, edited by M. Miasek (Amsterdam: Elsevier), p. 376.
[51] ALEKSEENO, M. V., and VEINGER, A. I., 1974, *Soviet Phys. Semicond.*, **8**, 143.
[52] DUNSTAN, D. J., NICHOLLS, J. E., CAVENETT, B. C., and DAVIES, J. J., 1980, *J. Phys.* C, **13**, 6409.
[53] HERMANN, C., and WEISBUCH, C., 1977, *Phys. Rev.* B, **15**, 823.
[54] VERITY, D., NICHOLLS, J. E., DAVIES, J. J., and BRYANT, F. J., 1980, *J. Phys.* C, **13**, L87.
[55] CAVENETT, B. C., EAVES, L., and SMITH, P. (to be published); see also BARANOV, P. G., *et al.*, 1977, *Soviet Phys. JETP Lett.*, **26**, 249.
[56] SCHNEGG, P. A., JACCARD, C., and AEGERTER, M., 1974, *Phys. Stat. Sol.* (*b*), **63**, 587.
[57] DAVIES, J. J., 1978, *J. Phys.* C, **11**, 1907.
[58] MANSON, N., and EDGAR, A., 1978, *Semicond. Insul.*, **4**, 209.
[59] KUHN, A., CHEVALIER, R., and RINSKY, A., 1975, *Acta crystallogr.* B, **31**, 2841.
[60] MERCIER, A., MOOSER, E., and VOITCHOVSKY, J. P., 1973, *J. Luminesc.*, **7**, 241.
[61] VOITCHOVSKY, J. P., and MERCIER, A., 1974, *Nuovo Cim.* (B), **22**, 273.
[62] KURODA, N., and NISHINA, Y., 1975, *Phys. Stat. Sol.* (*b*), **72**, 81.
[63] DAWSON, P., MORIGAKI, K., and CAVENETT, B. C., 1979, *Proceedings of the International Conference on Physics of Semiconductors*, Edinburgh, edited by B. L. H. Wilson (London: Institute of Physics), p. 1023.
[64] MORIGAKI, K., DAWSON, P., and CAVENETT, B. C., 1978, *Solid St. Commun.*, **28**, 829.
[65] CAVENETT, B. C., DAWSON, P., and MORIGAKI, K., 1979, *J. Phys.* C, **12**, L197.
[66] DAWSON, P., CAVENETT, B. C., MORIGAKI, K., and LEVY, F. (to be published).
[67] BREBNER, J. L., 1973, *Can. J. Phys.*, **51**, 497.
[68] MERCIER, A., and VOITCHOVSKY, J. P., 1975, *J. Phys. Chem. Solids*, **36**, 1411.
[69] DAWSON, P., KILLORAN, N., and CAVENETT, B. C., 1979, *Solid St. Commun.*, **32**, 1133.
[70] AULICH, E., BREBNER, J. L., and MOOSER, E., 1969, *Phys. Stat. Sol.*, **31**, 129.
[71] RAZBIRIN, B. S., KARAMAN, M. I., MUSHINSKII, V. P., and STARUKHIN, A. N., 1973, *Soviet Phys. Semicond.*, **7**, 753.
[72] BELENKII, G. L., and GODZHAEV, M. O., 1978, *Phys. Stat. Sol.* (*b*), **85**, 453.
[73] KILLORAN, N., CAVENETT, B. C., DAWSON, P., and LEVY, F. (to be published).
[74] THOMAS, D. G., GERSHENZON, M., and TRUMBORE, F. A., 1964, *Phys. Rev.* A, **133**, 269.
[75] DEAN, P. J., 1973, *Progress in Solid State Chemistry*, Vol. 8, edited by J. O. McCaldin and G. Somorjai (Oxford: Pergamon), p. 1.

[76] Cavenett, B. C., and Hagston, W. E., 1975, *Solid St. Commun.*, **16**, 1235.
[77] Dawson, P., and Cavenett, B. C., 1979, *J. Luminesc.*, **18/19**, 853.
[78] Dawson, P., Cavenett, B. C., and Sowersby, G., 1978, *Solid-St. Electron.*, **21**, 1451.
[79] Brunwin, R. F., Cavenett, B. C., Davies, J. J., and Nicholls, J. E., 1976, *Solid St. Commun.*, **18**, 1283.
[80] Dunstan, D. J., Cavenett, B. C., Dawson, P., and Nicholls, J. E. (to be published).
[81] Lambe, J., and Kikuchi, C., 1958, *J. Phys. Chem. Solids*, **9**, 492.
[82] Dielman, J., 1962, *Proc. Colloque Ampere*, Eindhoven (Amsterdam: North Holland), p. 412.
[83] Morigaki, K., 1964, *J. phys. Soc. Japan*, **19**, 1253.
[84] Patel, J. L., Nicholls, J. E., and Davies, J. J., 1981, *J. Phys.* C, **14**, 1339.
[85] Dang, Le Si, Lee, K. M., and Watkins, G. D., 1980, *Phys. Rev. Lett.*, **45**, 390.
[86] Dean, P. J., and Merz, J. L., 1969, *Phys. Rev.*, **178**, 1310.
[87] Merz, J. L., Nassau, K., and Shiever, J. W., 1973, *Phys. Rev.* B, **8**, 1444.
[88] Dunstan, D. J., Cavenett, B. C., Brunwin, R. F., and Nicholls, J. E., 1977, *J. Phys.* C, **10**, L361.
[89] Killoran, N., Cavenett, B. C., and Dean, P. J., 1981, *Solid St. Commun.*, **38**, 739.
[90] Dean, P. J., Venghaus, H., Pfister, J. C., Schaub, B., and Maxine, J., 1978, *J. Luminesc.*, **16**, 363.
[91] Toms, D. J., Helms, C. A., and Scott, J. F., 1978, *Phys. Rev.* B, **18**, 871.
[92] Tews, H., 1981, *Phys. Rev.* B, **23**, 587.
[93] James, J. R., Nicholls, J. E., Cavenett, B. C., Davies, J. J., and Dunstan, D. J., 1975, *Solid St. Commun.*, **17**, 969.
[94] James, J. R., Cavenett, B. C., Nicholls, J. E., Davies, J. J., and Dunstan, D. J., 1976, *J. Luminesc.*, **12/13**, 447.
[95] Shionoya, S., Koda, T., Era, K., and Fujiwara, H., 1964, *J. phys. Soc. Japan*, **19**, 1157.
[96] Era, K., Shionoya, S., and Washizawa, Y., 1968, *J. Phys. Chem. Solids*, **29**, 1827.
[97] Watkins, G. D., 1973, *Solid St. Commun.*, **12**, 589.
[98] Kasai, P. H., and Otomo, Y., 1962, *J. chem. Phys.*, **37**, 1263.
[99] Rauber, A., and Schneider, J., 1963, *Physics Lett.*, **3**, 230.
[100] Schneider, J., Holton, W. C., Estle, T. L., and Rauber, A., 1963, *Physics Lett.*, **5**, 312.
[101] Dischler, B., Rauber, A., and Schneider, J., 1964, *Phys. Stat. Sol.*, **6**, 507.
[102] Holton, W. C., de Wit, M., and Estle, T. L., 1966, *International Symposium on Luminescence*, edited by N. Kiehl and M. Kallmann (Munchen: Verlag Karl Thiemig), p. 454.
[103] Watts, R. K., 1973, *J. Mater. Sci.*, **8**, 1201.
[104] Nicholls, J. E., Davies, J. J., Cavenett, B. C., James, J. R., and Dunstan, D. J., 1979, *J. Phys.* C, **12**, 361.
[105] Dunstan, D. J., and Davies, J. J., 1979, *J. Phys.* C, **12**, 2927.
[106] Otomo, Y., and Kusumoto, H., 1966, *Proceedings of the International Conference on Luminescence*, Budapest, edited by G. Szigeti.
[107] Szigeti, G., Harsy, M., and Schanda, J., 1971, *Z. Naturf.* (a), **26**, 925.
[108] Rauber, A., and Schneider, J., 1966, *Phys. Stat. Sol.*, **18**, 125.
[109] Rauber, A., and Schneider, J., 1966, *Phys. Rev. Lett.*, **16**, 1075.
[110] Holton, W. C., and Watts, R. K., 1969, *J. chem. Phys.*, **51**, 1615.
[111] Davies, J. J., and Nicholls, J. E., 1979, *J. Phys.* C, **12**, 3329.
[112] Apple, E. F., and Williams, F. E., 1959, *J. electrochem. Soc.*, **106**, 224.
[113] Nicholls, J. E., and Davies, J. J., 1980, *J. Phys.* C, **13**, 2393.
[114] Schirmer, O. F., and Zwingel, D., 1970, *Solid St. Commun.*, **8**, 559.
[115] Zwingel, D., 1972, *J. Luminesc.*, **5**, 385.
[116] Baur, G., Freydorf, E. V., and Koschel, W. H., 1974, *Phys. Stat. Sol.* (a), **21**, 247.
[117] Shirmer, D. F., 1968, *J. Phys. Chem. Solids*, **29**, 1407.
[118] Cox, R. T., Block, D., Herve, A., Picard, R., Santier, C., and Helbig, R., 1978, *Solid St. Commun.*, **25**, 77.
[119] Block, D., Cox, R. T., Herve, A., Picard, R., Santier, C., and Halbig, R., 1977, *Semicond. Insul.*, **4**, 131.

[120] DUNSTAN, D. J., NICHOLLS, J. E., CAVENETT, B. C., DAVIES, J. J., and REDDY, K. V., 1977, *Solid St. Commun.*, **24**, 677.
[121] NICHOLLS, J. E., DUNSTAN, D. J., and DAVIES, J. J., 1977, *Semicond. Insul.*, **4**, 119.
[122] HOLTON, W. C., DE WIT, M., and ESTLE, T. L., 1966, *International Symposium on Luminescence*, edited by N. Kiehl and H. Kallmann (Munich: Verlag Karl Thiemig), p. 454.
[123] WATKINS, G. D., 1975, *Intrinsic Defects in II–VI Compounds* (ARL TR 75-0011) (Vancouver: National Technical Information Service).
[124] WATKINS, G. D., 1974, *Phys. Rev. Lett.*, **33**, 223.
[125] LEE, K. M., DANG, LE SI, and WATKINS, G. D., 1980, *Solid St. Commun.*, **35**, 527.
[126] LEE, K. M., DANG, LE SI, and WATKINS, G. D., 1980, *Proceedings of the International Conference on Defects and Radiation Effects in Semiconductors*, Oiso (to be published).
[127] REINBERG, A. R., HOLTON, W. C., DE WIT, M., and WATTS, R. K., 1971, *Phys. Rev.* B, **3**, 410.
[128] WATTS, R. K., HOLTON, W. C., and DE WIT, M., 1971, *Phys. Rev.* B, **3**, 404.
[129] DAVIES, J. J., and NICHOLLS, J. E., 1979, *J. Luminesc.*, **18/19**, 322.
[130] NICHOLLS, J. E., and DAVIES, J. J., 1979, *J. Phys.* C, 1917.
[131] VERITY, D., NICHOLLS, J. E., DAVIES, J. J., and BRYANT, F. J., 1980, *J. Phys.* C, **13**, L999.
[132] VERITY, D., DAVIES, J. J., NICHOLLS, J. E., and BRYANT, F. J., 1981, *J. appl. Phys.*, **52**, 737.
[133] GRIMMEISS, H. G., 1980, *New Developments in Semiconductor Physics*, (Lecture Notes in Physics, Vol. 122) (New York: Springer-Verlag), p. 50.
[134] KILLORAN, N., CAVENETT, B. C., PEAKER, A., HAMILTON, B., and DEAN, P. J. (to be published).
[135] BRUNWIN, R. F., HAMILTON, B., HODGKINSON, J., and PEAKER, A. R., 1981, *Solid-St. Electron.*, **24**, 249.
[136] KENNEDY, T. A., and WILSEY, N. C., 1978, *Phys. Rev. Lett.*, **41**, 977.
[137] DEAN, P. J., HENRY, C. H., and FROSCH, C. J., 1968, *Phys. Rev.*, **168**, 812.
[138] TOYOTOMI, S., and MORIGAKI, K., 1970, *J. phys. Soc. Japan*, **29**, 800.
[139] IL'IN, N. P., MASTEROV, V. F., SAMORUKOV, B. E., and SHTEL'MAKH, K. F., 1977, *Soviet Phys.*, **10**, 940.
[140] DEAN, P. J., and HENRY, C. H., 1968, *Phys. Rev.*, **176**, 928.
[141] MORGAN, T. N., 1978, *Phys. Rev. Lett.*, **40**, 190.
[142] MONEMAR, B., and SAMUELSON, L., 1976, *J. Luminesc.*, **12/13**, 507.
[143] KUKIMOTO, H., HENRY, C. H., and MERRITT, F. R., 1973, *Phys. Rev.* B, **7**, 2486.
[144] HENRY, C. H., KUKIMOTO, H., MILLER, T. L., and MERRITT, F. R., 1973, *Phys. Rev.* B, **7**, 2499.
[145] GRIMMEISS, H. G., LEDEBO, Z. A., OVREN, C., and MORGAN, T. N., 1974, *Proceedings of the International Conference on Physics of Semiconductors*, Stuttgart, edited by M. H. Pilkuhn (Stuttgart: Teubner), p. 386.
[146] GAL, M., CAVENETT, B. C., and SMITH, P., 1979, *Phys. Rev.*, **43**, 1611.
[147] GAL, M., CAVENETT, B. C., and DEAN, P. J., 1981, *J. Phys.* C, **14**, 1507.
[148] KOSCHEL, W. H., BISHOP, S. G., and MCCOMBIE, 1976, *Solid St. Commun.*, **19**, 521.
[149] STOCKER, H. J., and SCHMIDT, M., 1976, *J. appl. Phys.*, **47**, 2450.
[150] LIGHTOWLERS, E. C., and PENCHINA, C. M., 1978, *J. Phys.* C, **11**, L405.
[151] LIGHTOWLERS, E. C., HENRY, M. O., and PENCHINA, C. M., 1978, *Proceedings of the International Conference on Physics of Semiconductors*, Edinburgh, edited by B. L. H. Wilson (London: Institute of Physics), p. 307.
[152] KREBS, J. J., and STAUSS, G. H., 1977, *Phys. Rev.* B, **16**, 971.
[153] KREBS, J. J., and STAUSS, G. H., 1979, *Phys. Rev.* B, **20**, 795.
[154] WAGNER, R. J., and WHITE, A. M., 1979, *Solid St. Commun.*, **32**, 399.
[155] WHITE, A. M., 1979, *Solid St. Commun.*, **32**, 205.
[156] KILLORAN, N., CAVENETT, B. C., and HAGSTON, W. E., 1980, *Semi Insulating III–V Materials*, edited by G. J. Rees (Shiva: Nottingham), p. 190.
[157] KILLORAN, N., CAVENETT, B. C., and HAGSTON, W. E., 1980, *Solid St. Commun.*, **35**, 333.
[158] EAVES, L., ENGLERT, T. L., and UIHLEIN, C. L., *Proc. Oji Int. Seminar, Hakone* (to be published).

[159] LOWTHER, J. E., 1981, *Phil. Mag.* B. **43**, 61.
[160] BATES, C. A., ABHAVANI, A. S., and AUSTEN, S. P., 1980, *Semi Insulating III–V Materials*, edited by G. J. Rees (Shiva: Nottingham).
[161] VOILLOT, F., BARRAU, J., BROUSSEAU, M., and BRABANT, J. C., *J. Phys., Paris* (to be published).
[162] CLERJAUD, B., HENNEL, A. M., and MARTINEZ, G., 1980, *Solid St. Commun.*, **33**, 983.
[163] MOTT, N. F., DAVIS, E. A., and STREET, R. A., 1975, *Phil. Mag.*, **32**, 961.
[164] BIEGELSEN, D. K., and STREET, R. A., 1980, *Phys. Rev. Lett.*, **44**, 803.
[165] MOLLOT, F., CERNOGORA, J., and BENOIT A LA GUILLAUME, 1980, *J. non-crystalline Solids*, **35/36**, 930.
[166] DAVIS, E. A., 1979, *Amorphous Semiconductors* (Topics in Applied Physics, Vol. 36), edited by M. H. Brodsky (New York: Springer-Verlag), p. 41.
[167] SUZUKI, H., MURAYAMA, K., and NINOMIYA, T., 1979, *J. phys. Soc. Japan*, **46**, 693.
[168] DEPINNA, S. P., CAVENETT, B. C., AUSTIN, I. G., and SEARLE, T. M., 1980, *J. non-crystalline Solids*, **35/36**, 933.
[169] STREET, R. A., KNIGHTS, J. C., and BIEGELSEN, D. K., 1980, *Phys. Rev.* B, **18**, 1880.
[170] NASHASHIBI, T. S., AUSTIN, I. G., and SEARLE, T. M., 1977, *Phil. Mag.* B, **20**, 831.
[171] PAESLER, M. A., and PAUL, W., 1980, *Phil. Mag.* B, **41**, 393.
[172] PANKOVE, J. T., and CARLSON, D. L., 1979, *Appl. Phys. Lett.*, **31**, 450.
[173] AUSTIN, I. G., NASHASHIBI, T. S., SEARLE, T. M., LECOMBER, P. G., and SPEAR, W. E., 1979, *J. non-crystalline Solids*, **32**, 373.
[174] BRODSKY, M. H., TITLE, R. S., WEISER, K., and PETIT, G. D., 1970, *Phys. Rev.* B, **1**, 2632.
[175] MORIGAKI, K., DUNSTAN, D. J., CAVENETT, B. C., DAWSON, P., and NICHOLLS, J. E., 1978, *Solid St. Commun.*, **26**, 981.
[176] BIEGELSEN, D. K., KNIGHTS, J. C., STREET, R. A., TSANG, C., and WHITE, R. M., 1978, *Phil. Mag.* B, **37**, 477.
[177] LAMPEL, G., and SOLOMON, I. (private communication).
[178] DEPINNA, S., CAVENETT, B. C., AUSTIN, I. G., SEARLE, T. M., THOMPSON, M. J., ALLISON, J., and LECOMBER, P. G., *Phil. Mag.* (to be published).
[179] MOVAGHAR, B., RIES, B., and SCHWEITZER, L., 1980, *Phil. Mag.*, **41**, 141.
[180] FRIEDRICH, A., and KAPLAN, D., 1979, *J. Electron. Math.*, **8**, 79.
[181] STREET, R. A., 1980, *Phys. Rev.* B, **21**, 5775.
[182] DEPINNA, S., CAVENETT, B. C., AUSTIN, I. G., and SEARLE, T. M., *Solid St. Commun.* (to be published).
[183] KAPLAN, D., SOLOMON, I., and MOTT, N. F., 1978, *J. Phys. Leti., Paris*, **39**, L-51.
[184] LEE, K. M., DANG, LESI, WATKINS, G. D., and CHOYKE, W. J., 1981, *Solid St. Commun.*, **37**, 551.
[185] DEPINNA, S., CAVENETT, B. C., MONEMAR, B., and KILLORAN, N., *Phys. Rev.* (to be published).
[186] SMITH, P., CAVENETT, B. C., and SCHWAB, C. (to be published).
[187] LAMB, W. E., and CAVENETT, B. C. (to be published).
[188] GODLEWSKI, M., LAMB, W. E., and CAVENETT, B. C., *Solid St. Commun.* (to be published).
[189] GODLEWSKI, M., LAMB, W. E., and CAVENETT, B. C., *J. Phys.* C (to be published).
[190] GODLEWSKI, M., WILAMOWSKI, Z., KAMINSKA, M., LAMB, W. E., and CAVENETT, B. C 1981, *J. Phys.* C, **14**, 2835.
[191] TITLE, R. S., MANDEL, G., and MOREHEAD, F. F., 1964, *Phys. Rev.* A, **136**, 300.
[192] ABDULLAEVA, S. G., and MAMEDOV, H. S., 1977, *Phys. Stat. Sol.* (*a*), **40**, K7.